Contributions of the direct and statistical reaction mechanisms in scattering of fast neutrons by low-lying levels of light and medium nuclei

V. M. Bychkov, A. V. Ignatyuk, and V. P. Lunev

Physics and Power Institute, Obninsk

D. Seeliger, S. Unholzer, D. Schmidt, T. Streil, and D. Hermsdorf

Technical University, Dresden, GDR

Fiz. Elem. Chastits At. Yadra **14**, 373–419 (March–April 1983)

The main features in the behavior of the functions for excitation of low-lying nuclear levels by neutrons are analyzed and the connection between these features and the parameters of the optical and statistical models used to describe them is discussed. The differences between the dynamical-deformation parameters of nuclei derived from direct inelastic scattering of nucleons and from Coulomb excitation of low-lying collective levels are considered. It is shown that direct transitions make an important contribution to the excitation functions of individual levels even at comparatively low neutron energies. The part played by structural changes in the neutron strength functions in explaining the observed energy dependence of the inelastic-scattering cross sections in the near-threshold region is elucidated.

PACS numbers: 25.40.Fq, 24.60.Gv, 24.50. + g, 24.10.Ht

INTRODUCTION

Investigations of the interaction between neutrons and nuclei have been a subject of unflagging interest in all stages of the development of nuclear physics. In the first place, this is due to the specific properties of the neutron, which, in contrast to charged particles, can penetrate into a nucleus and induce nuclear reactions at an arbitrarily low kinetic energy. As a result, neutron absorption or scattering experiments are very informative for studying the resonance structure of nuclear-reaction cross sections and also the associated properties of excited nuclear states. As the energy of the incident neutrons is raised in such experiments, one can investigate in detail all the effects that arise on the transition from isolated to overlapping resonances and, at even higher energies, one can study the behavior of all the main components of the averaged description of the cross sections of nuclear reactions.

In the theoretical analysis of the interaction cross sections of various particles with nuclei, wide use is at present made of the division of the reaction mechanisms into fast direct processes, in which a comparatively small number of degrees of freedom in the nucleus are excited, and the slower statistical or compound processes, which are associated with the excitation of fairly complicated "long-lived" states of a compound nucleus.[1-4] Reactions for which one of these mechanisms is dominant are well known.[3,4] However, the situation when both mechanisms make comparable contributions to the observed cross sections is very common. A typical example of this situation is provided by the fast-neutron scattering cross sections considered in the present paper. We hope that the discussion of them will not only demonstrate the possibilities of the existing theoretical models in describing the experimental material accumulated in recent years but also draw to the attention of the experimentalists the data that, when obtained with more accuracy, will be of the greatest interest for the further development of our ideas about the mechanisms of nuclear reactions and the properties of highly excited nuclei.

1. THEORETICAL DESCRIPTION OF THE MECHANISMS OF ELASTIC AND INELASTIC SCATTERING OF NEUTRONS

Optical model and direct transitions. To analyze differential scattering cross sections, averaged over resonances, wide use is presently made of various modifications of the optical model of the nucleus.[5-7] In the simplest phenomenological formulation of this model, the interaction of the incident particle with the nucleus is approximated by a local complex single-particle potential whose imaginary part simulates in integrated form the inelastic processes accompanying the elastic scattering. For nucleons, the optical potential is generally chosen in the form

$$V(r) = -(V_v + iW_v) f_v(r) + 4ia_s W_s \frac{df_s(r)}{dr} + V_{so} \frac{\lambda_\pi^2}{r} \frac{df_{so}(r)}{dr} (\vec{l}\cdot\vec{\sigma}), \quad (1)$$

where V_v is the depth of the real part of the potential, W_v and W_s are the amplitudes of volume and surface absorption, V_{so} is the spin–orbit component of the potential, $\lambda\!\!\!^{-}_\pi$ is the pion Compton wavelength, and $f_i(r) = \{1 + \exp[(r - r_i A^{1/3})/a_i]\}^{-1}$ are the form factors of the corresponding parts of the potential.

Solving the problem of scattering of particles by the potential, we can determine the set of diagonal elements of the collision matrix or the S matrix and by means of them find the differential, $d\sigma_s(\theta)/d\Omega$, and integral, σ_s, cross sections of elastic scattering. In the optical model, the diagonal elements of the collision matrix also determine the transmission coefficients

$$T_{lj}(E_n) = 1 - |S_{lj}|^2, \quad (2)$$

which characterize the probability that a nucleus absorbs particles with given orbital, l, and total, j, angular momentum. Summing the contributions of all the angular momenta, we obtain the integral cross section for formation of the compound nucleus,

 0090-4759/83/020155-20$04.40

$$\sigma_c(E_n) = \pi\lambda_n^2 \sum_{l,j} (2j+1)\, T_{lj}, \tag{3}$$

and adding the elastic scattering cross section, we find the total particle–nucleus interaction cross section,

$$\sigma_t(E_n) = \sigma_s + \sigma_c = 2\pi\lambda_n^2 \sum_{l,j} (2j+1)\,(1 - \mathrm{Re}\, S_{lj}), \tag{4}$$

where $\lambda_n = \hbar/\sqrt{2\mu E_n}$ is the wavelength of the incident particles, and E_n is the energy of these particles in the center-of-mass system. The basic equations of the optical model and methods for solving them are presented in great detail in Refs. 5 and 6, and in many laboratories there are now programs that implement this model on computers.[7]

It was already noted in the early analyses of scattering cross sections that for nucleons of medium energies the imaginary part of the optical potential is much less than the depth of the real potential.[5] Under such conditions, the mean free path of the nucleon is comparable with the nuclear diameter, and this not only increases the "transparency" of the nucleus for the incident nucleon, but also raises the probability of direct nuclear reactions, which take place without formation of a long-lived compound nucleus. In many cases, the direct-reaction cross section can be successfully described in the framework of the distorted-wave Born approximation.[3] The equations of this method for the differential inelastic-scattering cross sections can be represented schematically in the form

$$\frac{d\sigma_{if}^{\lambda}(\theta)}{d\Omega} = \sum_{\mu} \Big| \sum_{j_i j_f} C_{j_i j_f}^{\lambda\mu}(\theta) \int_0^{\infty} u_i^*(r)\, F_{\lambda}(r)\, u_f(r)\, r^2\, dr \Big|^2, \tag{5}$$

where $C_{j_i j_f}^{\lambda\mu}$ are geometrical coefficients determined by the laws of composition of the angular momenta of the nucleon in the entrance, i, and exit, f, channels, $u(r)$ are the radial wave functions of the optical model, and $F_\lambda(r)$ is the form factor of the excited state of the target nucleus.

In the phenomenological approach based on the relations of the collective model,[8] the form factors of direct transitions are usually written in the form

$$F_{\lambda}(r) = \frac{\beta_{\lambda} R_0}{(2\lambda+1)^{1/2}} \frac{dV(r)}{dr}, \tag{6}$$

where β_λ is the amplitude of the collective excitations of the nucleus of given multipolarity λ. Using the relations (5) and (6) to analyze the inelastic-scattering cross sections of nucleons, we can investigate the distribution of the amplitudes β_λ over the spectrum of the excited states of the nucleus. On the basis of such an analysis, very extensive spectroscopic information has now been accumulated on the collective properties of the lowest levels of nuclei.[8] However, at higher energies there is as yet very sparse experimental information on the distribution of the deformation parameters $\beta_\lambda(U)$ and, therefore, on the part played by direct processes in the excitation of these levels.

The relations (5) determine the probability of direct transitions only in the first order of perturbation theory. If the coupling of the entrance and exit channels is sufficiently strong, then in analyzing the cross sections of direct reactions one must take into account the part played by transitions of higher order. The most systematic way of solving this problem is in the framework of the coupled-channel method.[3] In the practical realization of this method, the interaction of the incident particle with the nucleus is simulated by means of a generalized optical potential

$$V(\mathbf{r}, \xi) = V(r) + V_c(\mathbf{r}, \xi), \tag{7}$$

which includes not only the single-particle optical potential (1) but also the potential V_c, which couples the channels and depends on the coordinates ξ of the excited states of the nucleus. Since the coupling of the channels leads to a significant complication of the scattering problem, the analysis of experimental data is usually done with allowance for only a comparatively small number of channels corresponding to excitation of the low-lying levels of the target nucleus. In this case, the imaginary part of the generalized optical potential (7), as in the single-channel optical model, characterizes the integrated influence on the considered scattering channels of all the remaining reaction channels.

Strong coupling of the channels is manifested in the first place in collective excitations of nuclei, and the phenomenological generalized optical potential is chosen, as a rule, in the same form as the single-particle potential (1), but with form factors $f_i(r, \Omega) = [1 + \exp\{(r - R_i(\Omega))/a_i\}]^{-1}$ that depend on the collective variables, namely, the Eulerian angles and the deformation parameters of the nucleus. For rotational axisymmetric nuclei, the corresponding radii R_i can be written in the form

$$R_i(\theta') = r_i A^{1/3} [1 + \textstyle\sum_{\lambda} \beta_{\lambda} Y_{\lambda 0}(\theta')], \tag{8}$$

where θ' is the azimuthal angle around the symmetry axis of the nucleus, and β_λ is the equilibrium deformation parameter of the nucleus. The connection between the coordinate system of the deformed nucleus and the system with the fixed direction of motion of the incident particle can be found by means of rotation functions.[8] For vibrational nuclei, the radii R_i are approximated by the relations

$$R_i(\theta, \varphi) = r_i A^{1/3} [1 + \textstyle\sum_{\lambda\mu} \alpha_{\lambda\mu} Y_{\lambda\mu}(\theta, \varphi)], \tag{9}$$

where θ and φ are polar angles in an arbitrary coordinate system. The coefficients $\alpha_{\lambda\mu}$ in this case are related to the dynamical-deformation parameters β_λ by

$$\alpha_{\lambda\mu} = \frac{\beta_{\lambda}}{(2\lambda+1)^{1/2}} [b_{\lambda\mu} + (-)^{\mu} b_{\lambda-\mu}^{+}], \tag{10}$$

where $b_{\lambda\mu}^{+}$ and $b_{\lambda\mu}$ are the operators of creation and annihilation of vibrational excitations in the target nucleus.[8] Using the relations (8) or (9), we can expand the form factors $f_i(r, \Omega)$ with respect to spherical harmonics and find the explicit form of the channel coupling potential in (7) for rotational and vibrational nuclei.

The equations of the generalized optical model for the deformed optical potential introduced in this way have been discussed by many authors, and a detailed analysis of these equations together with references to the original papers can be found in Tamura's well-known review.[9] In recent years, programs that implement the relations of the generalized optical model have been

successfully developed in many laboratories,[7,10] and in international nuclear-data centers much work has been done on the testing and unification of such programs.[7]

On the basis of the generalized optical model one can determine not only the diagonal elements of the collision matrix but also the nondiagonal elements $S^{J\pi}_{nlj,n'l'j'}$, which characterize the cross sections for direct excitation of the corresponding levels:

$$\sigma^{\mathrm{dir}}_{n'}=\frac{\pi\lambda^2_n}{2(I_0+1)}\sum_{Jlj l'j'}(2J+1)|S^{J\pi}_{0lj,n'l'j'}|^2. \tag{11}$$

Here, J and π are the total angular momentum and the parity of the states of the system consisting of the target nucleus and the nucleon, and I_0 is the spin of the target nucleus. The nondiagonal elements also occur with the diagonal elements in the definition of the transmission coefficients:

$$T^{J\pi}_{nlj}(E_n)=1-\sum_{n'l'j'}|S^{J\pi}_{nlj,n'l'j'}|^2. \tag{12}$$

This relation makes it possible to find the transmission coefficients not only for the ground state but also for excited states, and at low energies of the incident neutrons the differences between them may be very appreciable.[11,12] Knowing the transmission coefficients, one can readily find in the generalized optical model the integrated cross section for absorption of particles by the the nucleus or, which is effectively the same thing, the cross section of the reactions that proceed through a compound-nucleus stage.

Scattering of neutrons involving a compound nucleus. To consider absorbed particles, the compound-nucleus model proposed by N. Bohr is generally used. The basis of this model is the assumption that there exists in the reaction a long-lived intermediate stage, during which the nucleus "forgets" the conditions of its formation and then decays in accordance with statistical laws independently of the initial conditions of formation of the compound nucleus.[1] Relations of such a model, formulated with allowance for the conservations laws for the angular momenta and also the statistical distributions of the widths for the competing decay channels of the compound nucleus, are well known as the Hauser–Feshback–Moldauer relations.[2,13] For the excitation cross sections of isolated levels, these relations can be written in the form

$$\sigma^{\mathrm{comp}}_{n'}=\frac{\pi\lambda^2_n}{2(2I_0+1)}\sum_{ljJ}(2J+1)\left\{\Theta^{J\pi}_{lj}(E_n)\frac{\sum_{l'j'}\Theta^{J\pi}_{l'j'}(E_{n'})F^{J\pi}_{ljl'j'}}{\sum_{n''l''j''}\Theta^{J\pi}_{l''j''}(E_{n''})}-\delta_{nn'}\left(\frac{\Theta^{J\pi}_{lj}}{2}\right)^2\right\}, \tag{13}$$

where $\Theta^{J\pi}_{lj}=2\pi\langle\Gamma^{J\pi}_{nlj}\rangle/D^{J\pi}$ are the transmission coefficients that characterize the ratio of the mean partial widths $\langle\Gamma^{J\pi}_n\rangle$ of the resonances to the distance $D^{J\pi}$ between the resonances, and $F^{J\pi}_{lj,l'j'}$ are corrections for the fluctuations of the widths. If the distribution of the partial decay widths is described by a χ^2_ν distribution with ν degrees of freedom and there are no correlations between the widths for the different decay channels, the correction for the fluctuation of the widths will be determined by

$$F^{J\pi}_{\beta\gamma}=\left(1+\frac{2}{\nu_\beta}\delta_{\beta\gamma}\right)\int_0^\infty dt\prod_\alpha\left(1+\frac{2t}{\nu_\alpha}\frac{\Theta^{J\pi}_\alpha}{\sum_{\alpha'}\Theta^{J\pi}_{\alpha'}}\right)^{-(\nu_\alpha/2+\delta_{\alpha\beta}+\delta_{\alpha\gamma})}. \tag{14}$$

The fluctuation correction increases the cross section of elastic scattering through the compound nucleus and simultaneously decreases the cross section of the inelastic processes. When there are only a few open channels, the decrease may be very appreciable.[13]

Although the relations (8) and (9) are comparatively simple from the computational point of view, various problems that have not yet received complete theoretical solution arise when they are used to analyze experimental data. In the first place, there is the problem of determining the connection between the transmission coefficients $\Theta^{J\pi}_{lj}$ and the transmission coefficients $T^{J\pi}_{lj}$ of the optical model, and also the question of correlation of the width in the different decay channels and the determination of the number ν_{lj} of degrees of freedom. A rigorous solution to these problems is known only for the region of comparatively low energies of the incident neutrons, which corresponds to isolated resonances in the nonaveraged reaction cross sections. Under these conditions, the distribution of the neutron widths satisfies the Porter–Thomas law ($\nu^{J\pi}_{lj}=1$), and the transmission coefficients $\Theta^{J\pi}_{lj}$ are related to the corresponding transmission coefficients of the optical model by

$$T^{J\pi}_{lj}=\Theta^{J\pi}_{lj}-(\Theta^{J\pi}_{lj})^2/4. \tag{15}$$

The situation is much more complicated for overlapping resonances. The connection between $\Theta^{J\pi}_{lj}$ and $T^{J\pi}_{lj}$ in this case can be represented in the form

$$T^{J\pi}_{lj}=\Theta^{J\pi}_{lj}-\sum_{n'l'j'}M^{J\pi}_{nlj,n'l'j'}, \tag{16}$$

but to determine the terms $M^{J\pi}_{\alpha\beta}$ we now need to know the correlation properties of the resonance amplitudes of the scattering matrix.[13,15] So far, these properties have not been studied at all well, and our knowledge of them is based, not on direct experimental information, but only on the results of statistical simulation of the resonance structure of neutron cross sections.[14,15] Such simulation showed that when sufficiently many channels are open correlation between the resonance parameters may lead to an effective canceling of the terms with different $M^{J\pi}_{nlj,n'l'j'}$. If it is assumed that this "suppression" of the M terms is a common property of the region of overlapping resonances, the Θ_{lj} can be directly identified with the transmission coefficients of the optical model.[15] However, the question of the effective number of degrees of freedom for the different decay channels remains open. For overlapping resonances, we do not have a rigorous determination of ν_{lj} and can only expect the number of degrees of freedom for the partial neutron widths to be bounded by the inequality $1\leqslant\nu_{lj}\leqslant 2$. On the basis of statistical simulation of the cross sections, a simple empirical relation for the effective number of channels was proposed in Ref. 16:

$$\nu^{J\pi}_{lj}=1+\sqrt{T^{J\pi}_{lj}}. \tag{17}$$

It should be borne in mind that this relation describes reasonably well only the general tendencies in the variation of the fluctuations of the neutron widths in the region of overlapping resonances and does not pretend to a high accuracy in the case of a small number of open

neutron channels.[15]

Initially, the Hauser–Feshbach–Moldauer relations were obtained under the assumption that there is no contribution of the direct-reaction mechanism. Later, it was shown[14,15] that the general structure of these relations is still maintained when direct processes are present. In such a case, it is merely necessary to determine the transmission coefficients with allowance for the contribution of the direct processes, and also to take into account in the corrections for the fluctuation of the widths the correlations of the widths in the channels associated with the direct transitions. These correlations will somewhat increase the fluctuation correction, but this is significant only when there is a small number of open channels strongly coupled to the direct transitions.[15] With increasing number of channels, the correlation effects rapidly become weaker, and there is a simple superposition of the cross sections of the direct reactions and reactions through the compound nucleus.

On the basis of our discussion of the methods for describing the cross sections of nuclear reactions averaged over the resonance structure, we can formulate a number of problems whose solution is topical in the study of the scattering of fast neutrons: 1) How must the parameters of the optical potential be chosen for a simultaneous analysis of the differential cross sections of elastic and inelastic scattering; 2) how good a description of the experimental data should we strive for, given the existing uncertainties in the parameters of the employed models; 3) given the existing uncertainties, how unique are conclusions about the relative contributions of the direct and compound scattering mechanisms at different neutron energies? The bulk of the present review will be devoted to answering these questions.

2. CHOICE OF THE PARAMETERS OF THE OPTICAL POTENTIAL

When the optical model is used to analyze the cross sections of nuclear reactions, one of two aims is usually being followed: 1) the achievement by a single "universal" set of optical-potential parameters of an optimal description of the observed scattering cross sections for a large number of nuclei; 2) the achievement of the best description of the differential cross sections of inelastic scattering and also the integral cross sections of inelastic interactions or the total reaction cross sections for a definite nucleus and a definite energy of the incident particles. Naturally, the physical content of the optical model will depend to some extent on the problem that is posed. In the first case, the parameters found for the optical model reflect the general variation of the single-particle average field of the nuclei and also the distribution of the probability of absorption of the nucleons in the nucleus determined by the imaginary part of the optical potential. But in the case of independent fitting of the parameters of the optical potential at each energy point, the optical model appears rather as a phenomenological method of parametrizing the properties of the collision matrix averaged over the energy. In this case, variations of the parameters with the energy, and also the fluctuations of the parameters of nearby nuclei, can be due not only to variations of the average field but also include various structural effects associated with the individual properties of the nuclei.

There have been many attempts by different authors to find a universal set of optical-potential parameters (see, for example, Refs. 5 and 6). At neutron energies above 14 MeV, the parameters found by Becchetti and Greenlees[17] from joint analysis of the differential cross sections of elastic scattering of protons and neutrons with energies up to 40 MeV have been widely used as such a set. Their parametrization was used to take into account the isotopic dependence of the real and imaginary parts of the potential, and also the variations in the depth of the potentials with the energy:

$$\left.\begin{aligned} &V_v = 56.3 - 24\,(N-Z)/A - 0.32E_n;\\ &W_v = (0.22E_n - 1.56) \text{ or } 0;\\ &W_s = 13.0 - 12.0\,(N-Z)/A - 0.25E_n;\\ &V_{so} = 6.2. \end{aligned}\right\} \qquad (18a)$$

The geometrical parameters were taken with somewhat differing values for the real, imaginary, and spin–orbit components of the potential:

$$\left.\begin{aligned} &r_v^{(R)} = 1.17;\ r_v^{(I)} = r_s = 1.26;\ r_{so} = 1.01;\\ &a_v^{(R)} = 0.75;\ a_v^{(I)} = a_s = 0.58;\ a_{so} = 0.75. \end{aligned}\right\} \qquad (18b)$$

All the quantities in (18a) are in mega-electron-volts and in (18b) in fermis.

The investigations of the differential cross sections of elastic neutron scattering made in Refs. 18–26 showed, however, that at neutron energies below 14 MeV the Becchetti–Greenlees parameters do not, as a rule, give a satisfactory description of the observed cross sections. In particular, for neutrons with energy 8 MeV a systematic analysis of the elastic-scattering cross sections was made by Holmqvist and Wiedling[18] for a large number of nuclei, and their description of the experimental data is shown in Fig. 1. The parameters of the optical potential corresponding to this description are shown in Fig. 2. It can be seen that not only the geometrical parameters but also the depths of the potentials that ensure the best reproduction of the observed angular distributions fluctuate very strongly from nucleus to nucleus. The amplitude of these fluctuations does not change significantly if the calculations of the optical potential are made with geometrical parameters averaged over the complete set of the analyzed nuclei and only the depths of the real and imaginary parts of the potential are varied (see the black circles in Fig. 2). Holmqvist and Wiedling proposed as a universal set in the range of neutron energies from 1.5 to 8 MeV the following parameters of the optical potential:

$$\left.\begin{aligned} &V_v = 44.44 + 0.1987A\\ &\quad - 1.893\cdot 10^{-3}A^2\\ &\quad + 4.527\cdot 10^{-6}A^3;\\ &W_s = 5.89\\ &\quad + 9.376\cdot 10^{-2}A\\ &\quad - 7.343\cdot 10^{-4}A^2\\ &\quad + 1.408\cdot 10^{-6}A^3;\\ &V_{so} = 8.0;\ r_v = r_{so}\\ &\quad = 1.183 + 3\cdot 10^{-4}A;\\ &r_s = 1.183 + 4\cdot 10^{-4}A;\\ &a_v = a_{so} = 0.66;\\ &a_s = 0.48. \end{aligned}\right\} \qquad (19)$$

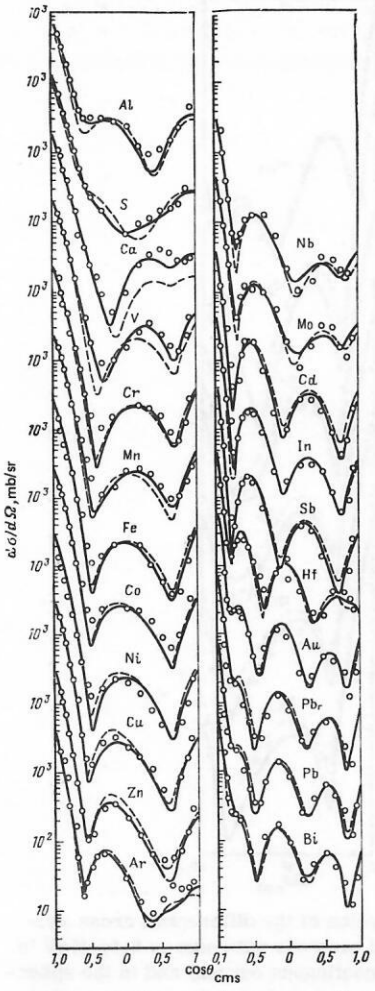

FIG. 1. Differential cross sections of elastically scattered neutrons with energy 8.05 MeV. The open circles are the experimental data, the continuous curves are the theoretical calculations with individually chosen parameters, and the broken curves are the calculations with the parameter set (19).

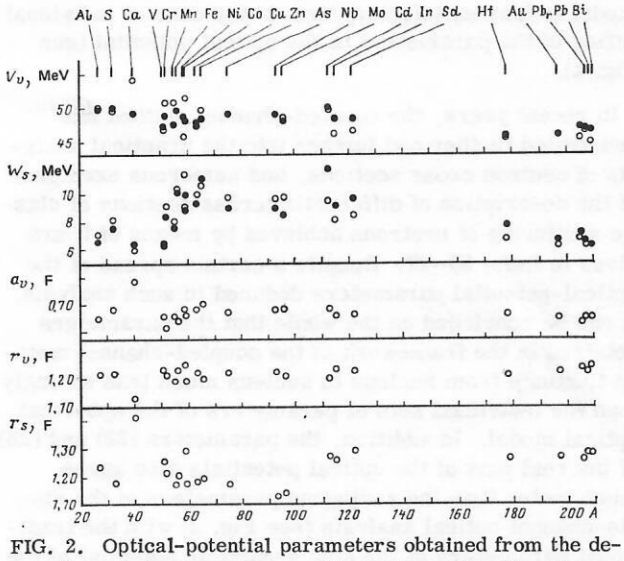

FIG. 2. Optical-potential parameters obtained from the description of elastic neutron scattering (see Fig. 1). The open circles are obtained in the case of fitting of all parameters of the potential, while the black circles are obtained for fixed geometrical parameters (19).

Calculations of the differential cross sections of elastic scattering of neutrons corresponding to these parameters are shown in Fig. 1. Although for each particular nucleus the deviation of the experimental data from the calculated curves for the parameter set (19) is somewhat larger than for individually chosen parameters, the description of the observed angular distributions by the common set of parameters is on the whole fairly good. As was shown in Ref. 19, the description of the experimental cross sections of elastic scattering at neutron energies 4.56 and 2.47 MeV is about as good.

Using in their analysis a more extensive set of experimental data on elastic scattering of polarized and unpolarized neutrons, Pasechnik *et al.*[20] obtained an entirely different set of parameters for the averaged optical potential for the same range of energies ($1.5 \leq E_n \leq 6.1$ MeV):

$$\left.\begin{aligned} &V_v = 48.7 - 0.33E_n;\ r_v = r_s = r_{so} = 1.25;\\ &W_s = 7.2 + 0.66E_n;\ a_v = a_{so} = 0.65;\\ &V_{so} = 7.5;\qquad\quad a_s = 0.47. \end{aligned}\right\} \tag{20}$$

The difference between the parameters (20) and (19) is partly due to the difference between the approaches to the selection of the experimental material—in Refs. 18 and 19, the results of the original measurements of the authors were mainly used, whereas in Ref. 20 all experimental data with comparable errors were taken into account in the analysis. In many cases, the extension of the analyzed data makes it possible to reduce appreciably the influence of systematic errors of individual measurements on the deduced parameters of the optical potential.

On the other hand, the difference between the parameters (19) and (20) reflects the ambiguity, noted by many authors, in the procedure for finding the parameters of the optical model (see Refs. 5, 6, and 18–20). It is helpful to express the interconnection between the variations of the energy and geometrical parameters of the optical potential in the form of the integral relations

$$\left.\begin{aligned} \mathcal{J}_v &= \frac{4\pi V_v}{A}\int_0^\infty f_v(r)\,r^2\,dr;\quad \mathcal{J}_s = \frac{4\pi W_s}{A}\int_0^\infty f_s(r)\,r^2\,dr. \end{aligned}\right\} \tag{21}$$

Sets of parameters that correspond to equal values of the integrals $\mathcal{J}_v$ and $\mathcal{J}_s$ give effectively equivalent descriptions of the experimental data.

The optical-potential parameters given above were found for the spherical optical model. At the same time, many of the analyzed nuclei have low-lying collective levels, which are excited very strongly in the direct inelastic-scattering mechanism. But at high intensities of the direct transitions the coupling of the elastic and inelastic scattering channels becomes important, and to study it we must go over from the single-channel to the generalized optical model.

In seeking the parameters of the generalized optical potential it is evidently best as a first approximation to use the parameters of the spherical potential found for magic nuclei. In such nuclei, the effects of the channel coupling are much weaker than in nonmagic nuclei, and this is a very favorable condition for studying the energy and isotopic dependence of the parameters of the potential. For nuclei with closed neutron, $N=50$, or

proton, $Z=50$, shell, a detailed investigation of the differential cross sections of elastic scattering of neutrons at energies from 7 to 26 MeV was made in Ref. 21. From the analysis of these data, and also the observed energy dependence of the total neutron cross sections for the tin isotopes in the region of neutron energies up to 15 MeV, the following parameters of the optical potential were obtained:

$$\left.\begin{aligned} &V_v = 54.2 - 22\,(N-Z)/A - 0.32E_n; \\ &W_s = 3.0 - 14\,(N-Z)/A + 0.51E_n; \\ &W_v = 0;\ r_v = 1.2;\ a_v = 0.7;\ r_s = 1.25;\ a_s = 0.65. \end{aligned}\right\} \quad (22)$$

For the spin–orbit part of the potential, the parameters $V_{so}=6.2$, $r_{so}=1.01$, and $a_{so}=0.75$ were chosen, and these were not varied in the process of describing experimental data. The parameters found for nuclei with a closed neutron shell ($N=50$) differed from (22) only by slight changes in the geometrical characteristics of the optical potential. When (20) and (22) are compared with the sets of parameters (18) and (19), the most striking thing is the appreciable difference between the energy dependences of the imaginary part of the optical potential. As will be shown below, the correct determination of this dependence is extremely important for analyzing the part played by direct processes at neutron energies below 7 MeV.

The main differences between the descriptions of the differential cross sections of elastic scattering of neutrons in the spherical and generalized optical models can be demonstrated by means of the results shown in Fig. 3. The calculations shown here for both models were made with the same set of optical-potential parameters,

$$\left.\begin{aligned} &V_v = 51.85 - 24\,(N-Z)/A - 0.33E_n;\ W_s = 2.55\sqrt{E_n}; \\ &W_v = 0;\ W_{so} = 7.0; \\ &r_v = r_s = r_{so} = 1.25;\ a_v = a_{so} = 0.65;\ a_s = 0.48, \end{aligned}\right\} \quad (23)$$

and for the generalized optical model the dynamical-deformation parameters β_λ for the lowest quadrupole and octupole excitations were taken on the basis of the available experimental data on direct reactions and Coulomb excitation of low-lying levels of even–even nuclei.[22] For odd nuclei, the model of weak coupling of the odd particle to the collective quadrupole phonons of the even–even core (the core-excitation model)[8] was used in the given calculations.

Comparing Figs. 1 and 3, we can conclude that for the even–even S, Cr, Fe, Ni, and Zn nuclei, in which the relations of the phenomenological collective model reproduce the properties of the low-lying collective levels comparatively well, the description of the experimental data in the generalized optical model with the unified set of parameters (23) is approximately the same as in the spherical optical model with individually fitted parameters. A similar conclusion will hold for the odd Cu and Nb nuclei, in which the core-excitation model agrees reasonably well with the observed schemes of the low-lying levels. But the core-excitation model does not reproduce the experimental spectra of the levels in the Mn, Co, and As isotopes nearly so well, and from the data given in Fig. 3 it can be seen that it is precisely for these isotopes that the description of the

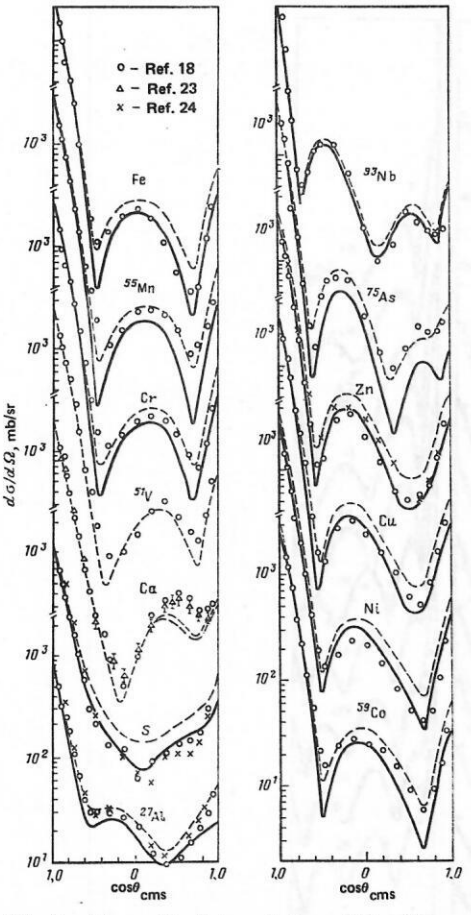

FIG. 3. Theoretical description of the differential cross sections of elastically scattered neutrons with energy 8.05 MeV in the coupled-channel model (continuous curves) and in the spherical optical model (broken curves) with the parameter set (23).

angular distributions in the adopted coupled-channel model is less satisfactory than in the case of individual fitting of the parameters of the optical potential (see Fig. 1).

In recent years, the coupled-channel method has penetrated further and further into the practical analysis of neutron cross sections, and numerous examples of the description of differential cross sections of elastic scattering of neutrons achieved by means of it are given in Refs. 25–27. Despite a certain spread of the optical-potential parameters deduced in such analysis, it can be concluded on the whole that the parameters obtained in the framework of the coupled-channel method fluctuate from nucleus to nucleus much less strongly than the individual sets of parameters of the spherical optical model. In addition, the parameters (22) and (23) of the real part of the optical potentials also agree much better than the analogous parameters of the single-channel optical analysis (see Fig. 2) with the traditional parameters of the single-particle potential of the shell model. This agreement between the results is one of the important achievements of the generalized optical model.

3. ON THE DIFFERENCES BETWEEN THE DYNAMICAL-DEFORMATION PARAMETERS IN INELASTIC NUCLEON SCATTERING AND COULOMB EXCITATION OF NUCLEI

At energies of the incident neutrons above 7 MeV in medium and heavy nuclei, the total number of open decay channels of the compound nucleus is so great that scattering through the compound nucleus does not make any significant contribution to the observed excitation cross sections of the low-lying levels. Under these conditions, the cross sections of inelastic scattering by low-lying levels are entirely determined by the direct transitions, and their analysis becomes a very effective tool for studying the characteristics of collective excitations of nuclei.

At the present time, the bulk of the data on the collective properties of nuclei is extracted from the analysis of Coulomb excitation of low-lying levels. In accordance with the ideas of the collective model of the nucleus, the reduced probability of the corresponding electric γ transitions is related to the dynamical-deformation parameters (10) of the nuclei by

$$B(E\lambda, 0^+ \to \lambda^\pi) = [(3/4\pi)\, ZeR_0^\lambda]^2 \beta_\lambda^2. \qquad (24)$$

The systematics of the deformation parameters obtained on the basis of this expression have been discussed on many occasions.[28,29] Usually, it is assumed that the same values of the parameters also determine the cross sections of the direct reactions of inelastic scattering of particles by low-lying collective levels. From the point of view of the microscopic approach, this assumption is not sufficiently rigorous, since it does not take into account the differences between the excitation of the isoscalar and isovector components of the form factors of nuclear transitions. The origin of such differences can be readily followed in the example of valence transitions in the simplest shell model.

For nuclei with a closed neutron shell, low-frequency excitations can be formed only from proton transitions, and since the two-particle effective forces for nonidentical nucleons are much greater than for identical nucleons, the form factors of the direct transitions in such nuclei must be appreciably greater for the (n, n') reaction than for the (p, p'). At the same time, the opposite picture must be observed for nuclei with a closed proton shell. This is a simplified example, and in real nuclei the polarization of the nucleons in the closed shells has an influence on the intensity of the valence transitions. However, the main qualitative features of the considered differences between the form factors of the inelastic scattering of protons and neutrons remain when polarization effects are taken into account. A quantitative analysis of the differences expected in this case between the dynamical-deformation parameters for electromagnetic excitations of nuclei and inelastic scattering of nucleons was made in Ref. 30.

The theoretically predicted differences between the nuclear and electromagnetic deformation parameters were confirmed by recent very accurate experimental investigations of the cross sections of inelastic scattering of neutrons by near-magic nuclei.[21,31] These experiments measured to high accuracy the differential cross sections for elastic and inelastic scattering of 11-MeV neutrons by the nuclei ^{88}Sr, ^{90}Zr, and ^{92}Mo, which have a closed neutron shell, $N = 50$, and also by the tin isotopes ^{116,118,120,122,124}Sn, which correspond to a closed proton shell, $Z = 50$. The results of these measurements for the tin isotopes are given in Fig. 4 together with the theoretical description of the observed cross sections.[31] Analysis of the elastic-scattering cross sections made it possible to determine fairly reliably the parameters of the optical potential for each of the considered nuclei, and subsequent description of the inelastic-scattering cross sections in the framework of the distorted-wave Born approximation made it possible to determine the quadrupole-deformation parameters $\beta_2^{(n)}$. The deformation parameters found in this way are given in Table I. This table also contains the experimental values of the deformation parameters obtained by the analysis of the cross sections of inelastic proton scattering, $\beta_2^{(p)}$, and the description of Coulomb excitation: $\beta_2^{(\gamma)}$. Although in many cases the errors in the deduced deformation parameters are comparable with the expected differences between the parameters, the available data nevertheless make it possible to speak with confidence of a systematic difference between the parameters $\beta_2^{(n)}$, $\beta_2^{(p)}$, and $\beta_2^{(\gamma)}$, and these differences are in good agreement with the results of the theoretical analysis of the nuclear and electromagnetic deformation parameters given in Table I.

The above theoretical estimates of the dependence of the deformation parameters on the method of excitation of the nuclei were obtained on the basis of the simplest schematic model of polarization effects, when all high-frequency core excitations are concentrated in two collective modes—the isoscalar and isovector quadrupole giant resonances.[30] The shortcomings of this approximation can be eliminated by analyzing the form factors of the nuclear transitions in the framework of more realistic microscopic models. Such an analysis was made for an effective interaction of the nucleons represented in the form of separable multipole forces matched to the real average field of the nuclei.[32] Such

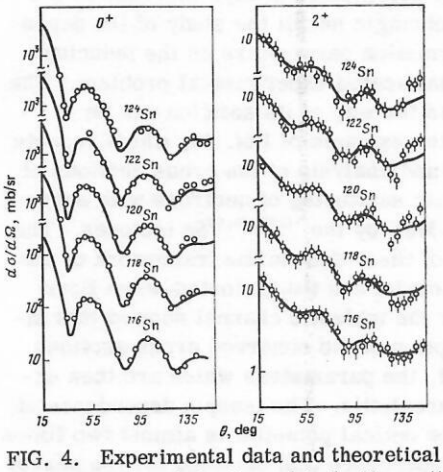

FIG. 4. Experimental data and theoretical description of the cross sections of elastic and inelastic scattering of 11-MeV neutrons for tin isotopes.

TABLE I. Quadrupole dynamical-deformation parameters deduced from the excitation of the lowest 2^+ levels of nuclei with a closed neutron, $N=50$, or proton, $Z=50$, shell (Ref. 27).

Deformation parameters		Nuclei with $N=50$			Nuclei with $Z=50$				
		^{88}Sr	^{90}Zr	^{92}Mo	^{116}Sn	^{118}Sn	^{120}Sn	^{122}Sn	^{124}Sn
Experiment[21,31]	$\beta_2^{(n)}$	0.133 (7)	0.085 (8)	0.099 (5)	0.120 (10)	0.109 (7)	0.106 (5)	0.100 (6)	0.092 (6)
	$\beta_2^{(p)}$	0.11	0.070 (5)	0.080 (6)	0.133	0.134 (10)	0.119 (10)	0.112 (7)	0.108 (7)
	$\beta_2^{(n)}/\beta_2^{(p)}$	1.2	1.2	1.3	0.90	0.81	0.90	0.90	0.85
	$\beta_2^{(\gamma)}$	0.14 (2)	0.094 (5)	0.116 (8)	0.118 (7)	0.108 (2)	0.106 (2)	0.102 (2)	0.096 (2)
Theory[30]		$\beta_2^{(\gamma)} > \beta_2^{(n)} > \beta_2^{(p)}$			$\beta_2^{(\gamma)} < \beta_2^{(n)} < \beta_2^{(p)}$				
	$\beta_2^{(n)}/\beta_2^{(p)}$	1.35	1.33	1.31	0.88	0.89	0.90	0.90	0.91
	$\beta_2^{(\gamma)}$	0.15	0.093	0.109	0.105	0.093	0.099	0.094	0.084

*The numbers in the brackets give the errors in the last decimal place of the experimental values of the deformation parameters.

forces are widely used to describe the collective properties of nuclei,[8] and by means of them it is possible to reproduce very well all the main features of the observed spectral distributions of the intensities of low- and high-frequency excitations. For the ratio $\beta_2^{(n)}/\beta_2^{(p)}$ of the deformation parameters the values 1.08–1.12 were obtained in this analysis for nuclei with $N=50$ and 0.90–0.94 for the tin isotopes.[32] Although these numbers are somewhat smaller than the estimates of the schematic model (see Table I), the general systematic difference between the quadrupole-deformation parameters in the considered groups of nuclei persists in a very stable manner when the theoretical description is varied.

When we move away from the magic numbers, we must expect a weakening of the shell effects and a corresponding decrease in the difference between the deformation parameters for the different fields that induce the nuclear transitions. Since the absolute values of the deformation parameters always increase at the same time, for nonmagic nuclei the study of the dependence of the deformation parameters on the inducing field is a very complicated experimental problem. The main difficulties in the way of its solution can be demonstrated by the example of Ref. 33, which reports the measurement and analysis of the cross sections of elastic and inelastic scattering of neutrons with energies 6, 8, and 10 MeV by the ^{76,78,80,82}Se isotopes. The original analysis of these data in the framework of the spherical optical model and the distorted-wave Born approximation for the inelastic channel showed that although the description of the observed cross sections can be fairly good, the parameters which are then extracted are too unrealistic. The isospin dependence of the real part of the optical potential is almost two times weaker than the dependence (22) obtained for the nearby nuclei, whereas the quadrupole-deformation parameters are several times larger than in the description of Coulomb excitation.

These difficulties can be eliminated to a considerable degree if the elastic and inelastic scattering cross sections are analyzed on the basis of the coupled-channel method. For 8-MeV neutrons, the description of the experimental data obtained in this method is given in Fig. 5, and the corresponding quadrupole-deformation parameters are given in Table II together with the parameters found by analyzing the inelastic scattering of protons[34] and the data of experiments on electromagnetic excitation.[35] According to the results of the proton investigations, we have in the selenium isotopes differences between the nuclear and Coulomb deformation parameters of the same sign, $\beta_2^{(\gamma)} > \beta_2^{(p)}$, as in the nuclei considered above with a closed neutron shell, $N=50$. At the same time, the ratio $\beta_2^{(\gamma)}/\beta_2^{(p)}$ increases with the filling of the shell, approaching the values given in Table I. On the basis of the available data, it is still difficult to understand what conclusions should be drawn from the results of the neutron experiments. The deduced parameters $\beta_2^{(n)}$ may, in addition to the statistical errors of the analysis indicated in Table II, be also distorted by the systematic errors associated with the choice of the optical potential. To eliminate such errors, it is necessary to investigate the differential

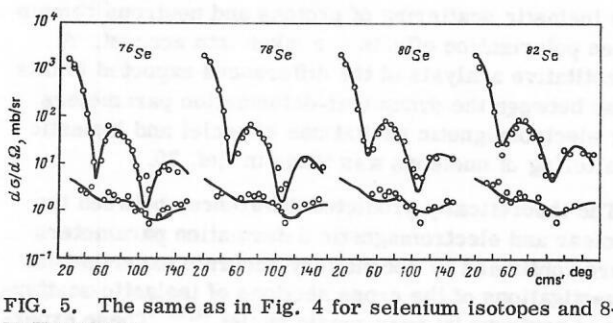

FIG. 5. The same as in Fig. 4 for selenium isotopes and 8-MeV neutrons.

TABLE II. Quadrupole-deformation parameters for the first 2^+ levels of selenium isotopes (references are given in square brackets).

Isotope	$\beta_2^{(n)}$ [33]	$\beta_2^{(p)}$ [34]	$\beta_2^{(\gamma)}$ [35]
^{76}Se	0.28 (1)	0.278 (7)	0.310 (2)
^{78}Se	0.27 (1)	0.243 (6)	0.268 (3)
^{80}Se	0.25 (1)	0.210 (5)	0.232 (2)
^{82}Se	0.22 (1)	0.159 (4)	0.192 (2)

cross sections of inelastic neutron scattering in a wider range of energies of the incident neutrons and, evidently, only on the basis of the results of such investigations will it be possible to draw reliable conclusions about the differences between $\beta_2^{(n)}$ and $\beta_2^{(p)}$.

The foregoing was entirely concentrated on the quadrupole-deformation parameters, which determine the intensities of direct excitation of the lowest 2^+ levels of even–even nuclei. A similar dependence of the dynamical-deformation paramaters on the inducing external field can be expected in the case of direct excitation of higher levels or levels of different multipolarity. Comparatively extensive experimental information is now available on direct excitation of the first octupole levels of even–even nuclei for scattering of various particles.[8,29,35,36] Unfortunately, the errors in the octupole-deformation parameters then deduced are in the majority of cases still so large that on their basis no unambiguous conclusions can be drawn about the differences between the nuclear and Coulomb deformation parameters. Experimental data on transitions with high multipolarity $\lambda \geq 4$ are very sparse. Although a systematic theoretical analysis of such transitions has not yet been made, it can be expected from the general ideas of the microscopic approach that for the corresponding, comparatively weakly collectivized levels the differences between the effective deformation parameters for different particles will be significantly greater than for the lowest, strongly collectivized quadrupole and octupole levels. Experimental investigations of these differences would be of considerable interest, both for the study of the structure of multipole excitations and for the analysis of the integrated contribution of direct transitions in the various nuclear reactions.

4. ANALYSIS OF THE DIFFERENTIAL CROSS SECTIONS OF INELASTIC SCATTERING OF NEUTRONS BY LIGHT NUCLEI

Above, we have considered nuclei for which the direct mechanism of excitation of the low-lying levels is predominant at energies of the incident neutrons above 6 MeV. If at the same energies we go over to lighter nuclei, then in them scattering through the compound nucleus becomes important as well as the direct mechanism. Analyzing the angular distributions of the scattered neutrons, we can investigate the energy dependence of the contributions of both mechanisms. Particularly favorable for this is the region of mass numbers $20 < A < 40$, in which one can more readily than in medium and heavy nuclei distinguish experimentally the excitation functions of individual levels, while at the same time the observed neutron cross sections are still averaged over a fairly large number of compound-nucleus resonances.

Among the light nuclei, the isotope ^{28}Si has been studied in most detail; for it, measurements and an analysis of the differential cross sections of elastic and inelastic scattering of neutrons by the first 2^+ level ($Q = -1.779$ MeV) in the range of energies of the incident neutron from 6 to 15 MeV were made in Refs. 37–44, while in Refs. 43 and 44 the excitation cross sections of higher levels were also studied. The observed elastic-scattering cross sections and their theoretical description are shown in Fig. 6.[44] Similar data on the cross section for inelastic scattering of neutrons by the 2^+ level are given in Fig. 7, and Fig. 8 shows data on the cross sections of inelastic scattering by the levels 4^+ ($Q = -4.618$ MeV) and 0^+ ($Q = -4.979$ MeV).

In the theoretical analysis of the scattering cross sections, the possibility of describing the experimental data on the basis of the spherical optical model was first investigated. The optical-potential parameters found from the description of the differential cross sections of inelastic scattering of 10-MeV neutrons[41] were used. It can be seen from the results of the calculations given in Fig. 6 that with these parameters it is possible to achieve a fairly good description of the observed elastic-scattering cross sections for the com-

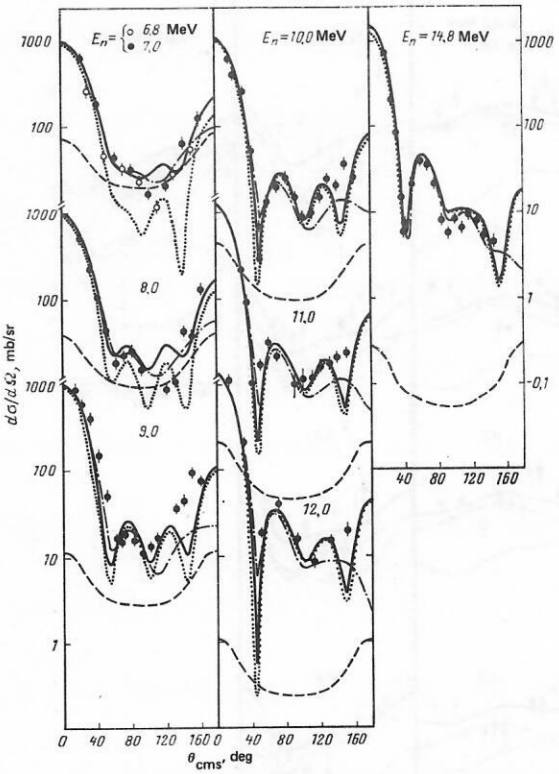

FIG. 6. Differential cross sections for elastic scattering of neutrons by the isotope ^{28}Si (the points) and the different components in their theoretical description. The broken curves are the cross sections for scattering through the compound nucleus; the dotted curves, the cross sections of potential scattering in the coupled-channel model; the continuous curves, the total cross sections of the two scattering mechanisms in the coupled-channel model; and the chain curves, the analogous cross sections in the spherical optical model.

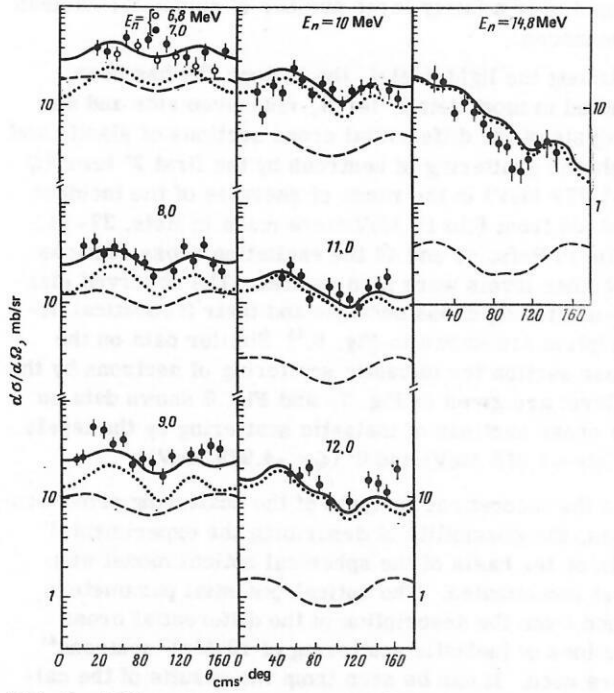

FIG. 7. Differential cross sections for inelastic scattering of neutrons by the first 2^+ level of the nucleus ^{28}Si. The theoretical curves are the same as in Fig. 6.

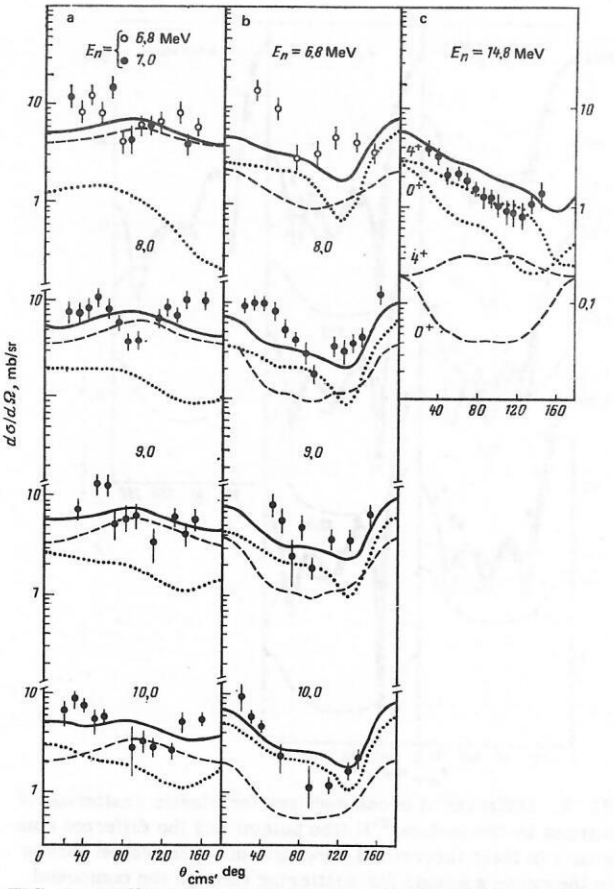

FIG. 8. Differential cross sections for inelastic scattering of neutrons by the levels 4_1^+ (a) and 0_2^+ (b) of the nucleus ^{28}Si. For neutrons with energy 14.8 MeV (c), the experimental points and the continuous theoretical curve describe the total cross section of scattering by both levels. The remaining curves are the same as in Fig. 6.

plete range of energies of the incident neutrons from 7 to 14 MeV. However, difficulties arise when this optical potential is used to analyze the inelastic cross sections. On the one hand, excessively large quadrupole-deformation parameters are needed in the description in the distorted-wave Born approximation of the cross sections of direct excitation of the first 2^+ level in the region of energies $E_n > 10$ MeV.[41] At the same time, the cross section of inelastic scattering through the compound nucleus is too large at low energies, this being manifested especially clearly in the analysis of the excitation cross sections of the levels 4_1^+ and 0_2^+.[44]

If we go over to the coupled-channel model, then to describe the experimental data we must above all reduce the imaginary part of the optical potential. These changes characterize the part played by the inelastic reaction channels taken into account in the redistribution of the flux of incident neutrons, and the depth of the imaginary part of the potential decreases more strongly, the larger the number of channels included in the coupling scheme. In the calculations, we adopted the rotational coupling scheme of the levels $0_1^+-2_1^+-4_1^+$, and to it added the vibrational coupling scheme of the levels $0_1^+-0_2^+$. This required a decrease in the imaginary part of the optical potential by almost two times. The resulting description of the angular distribution of elastically scattered neutrons differs overall very little from the description in the framework of the spherical optical model (see Fig. 6). Much more important is the consistency obtained in the coupled-channel model in the results of the analysis of the inelastic neutron-scattering cross sections. The decrease in the imaginary part of the potential significantly decreases the cross sections of elastic and inelastic scattering of the neutrons through the compound nucleus, and this agrees well with the experimental data at neutron energies 7 and 8 MeV, where an appreciable contribution of the compound scattering mechanism is observed.

It should be noted that for neutrons with energy 7–8 MeV the analysis of the differential elastic-scattering cross sections in the region of the deep minimum ($\theta \approx 110°$) makes it possible to investigate the part played by overlapping of resonances in the description of the correction (14) for the fluctuation of the neutron widths. The cross section at the minimum is almost completely determined by scattering through the compound nucleus, and by analyzing the observed cross sections we can find the mean value $\overline{F}$ of the correction for the elastic channel. Since the total number of open decay channels of the compound nucleus at these energies is fairly large, the corresponding correction must approach its maximal value: $F_{nn} = 3$ in the absence of correlation between the resonance parameters and $F_{nn} = 2$ for strongly overlapping correlated resonances.[13-15] The value of the correction needed to describe the experimental data, $\overline{F}_{nn} \approx 1.6-1.8$,[40] is very close to the expected mean value of the correction for strongly overlapping resonances, and this result is an experimental confirmation of the need to take into account the correlation of the resonance parameters in calculations of the mean cross sections of neutron reactions. The required fluctuation increase in the elastic-scattering

cross section is well reproduced in calculations that use the relation (17) to determine the number of open channels, which can be taken as additional evidence for the effectiveness of this very simple simulation of the statistical properties of the neutron widths.

In calculations of the cross sections of direct inelastic neutron scattering a very important question is the choice of the deformation parameters that determine the form factors (8) of direct excitation of collective levels. The rotational nature of the lowest levels of the ^{28}Si nucleus is usually identified on the basis of the observed intensity of the $E2$ transitions,[45] and also the results of analysis of the differential cross sections for inelastic scattering of charged particles.[46-49] However, the equilibrium-deformation parameters are then deduced with a very great uncertainty. The origin of this situation can be readily understood from the description of the cross sections for scattering of 10-MeV neutrons by the levels 0^+, 2^+, and 4^+ of the rotational band given in Fig. 9. The theoretical curves were obtained for two sets of parameters β_2 and β_4 corresponding to an elongated cigar-shaped ($\beta_2 > 0$) and oblate lens-shaped ($\beta_2 < 0$) nucleus. Neither the elastic-scattering cross sections nor the angular distributions of inelastic scattering of neutrons by the first 2^+ level are sensitive to the choice of the sign of the equilibrium deformation, and it is only the data on the excitation of the 4^+ level that to some extent distinguish the alternative sets of parameters.

Since an analogous conclusion also applies to the differential scattering cross sections of charged particles, to determine the deformation parameters data on the asymmetry of the scattering of polarized protons were used in Refs. 47 and 48 in addition to the inelastic-scattering cross sections. As a result of joint analysis of these data for 20.3-MeV protons the parameters $\beta_2 = -0.55$ and $\beta_4 = 0.33$ were obtained,[47] whereas for 24.5-MeV protons the values were $\beta_2 = -0.40$ and $\beta_4 = 0.10$.[48] In Ref. 49, for the range of incident-proton energies from 14 to 40 MeV, data on the probability of proton spin flip during scattering were used as well as the inelastic-scattering cross sections. The hexadecapole-deformation parameters then found depend rather strongly on the proton energy, varying from $\beta_4 \approx 0.35$–0.40 at 14 MeV to $\beta_4 = 0.15$ for high-energy protons. The quadrupole-deformation parameters varied much less—from $\beta_2 = -0.4$ to -0.5 at proton energies below 20 MeV to $\bar{\beta}_2 = -0.37 \pm 0.05$ for high-energy protons.

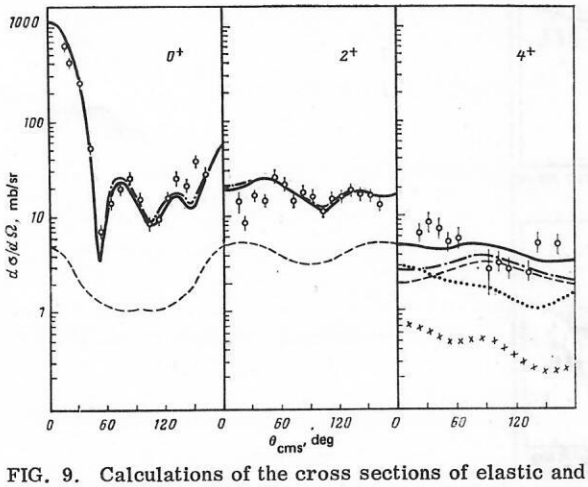

FIG. 9. Calculations of the cross sections of elastic and inelastic scattering of neutrons with energy 10 MeV under different assumptions about the equilibrium deformation of the nucleus ^{28}Si. The continuous curves correspond to $\beta_2 = 0.48$ and $\beta_4 = -0.30$; the chain curves, to $\beta_2 = -0.48$ and $\beta = 0.10$. For the 4^+ level, the cross sections of the direct processes corresponding to the two assumptions are also given (dotted curve and the crosses).

The energy dependence of the deformation parameters evidently reflects the inadequacies of the rigid-rotator model used to analyze the experimental data. The observed ratio of the energies of the rotational band, $E_{4+}/E_{2+} = 2.59$, like the ratio of the reduced probabilities of the $E2$ transitions, $B(E2; 4^+ \to 2^+)/B(E2; 2^+ \to 0^+) = 1.06 \pm 0.14$,[45] differs appreciably from the values corresponding to the rigid-rotator model: $(E_{4+}/E_{2+})^{\text{rot}} = 3.33$ and $B(E2; 4^+ \to 2^+)/B(E_2; 2^+ \to 0^+) = 1.43$. Ignoring these differences when analyzing the inelastic-scattering cross sections, we deduce somewhat distorted values of the deformation parameters, and the variations of the parameters with the energy characterize the possible distortions.

The influence of the deviations from the coupled-channel scheme of the rigid-rotator model on the differential cross sections of direct inelastic scattering of neutrons was investigated in Refs. 43 and 44, in which it was found that a decrease in the coupling of the 2_1^+ and 4_1^+ levels with a simultaneous increase in the hexadecapole-deformation parameter leads to a general improvement in the description of the observed angular distributions for scattering of neutrons by the 2_1^+ and 4_1^+ levels for the complete range of energies of incident neutrons from 7 to 14.8 MeV. The deformation parameters $\beta_2 = 0.48$ and $\beta_4 = -0.30$ then obtained are close in absolute magnitude to the values obtained from the differential cross sections for scattering of protons of comparable energies.[47,49] The signs of the deformation parameters were chosen on the basis of an analysis of the excitation cross sections of the level 4_1^+, but in view of the uncertainties in the analysis mentioned above great significance should not be attached to this choice. Given the existing errors in the neutron cross sections, it is still impossible to fix all the parameters of the optical potential, and the values found for the deformation parameters in fact include the possible errors in the determination of the remaining parameters. These errors can be eliminated by increasing the reliability of the measurements of the differential cross sections of elastic and inelastic neutron scattering, i.e., by obtaining experimental data with accuracy comparable to that of the data given in Figs. 4 and 5.

However, the existing uncertainties in the choice of the parameters of the generalized optical model are not very important for the determination of the ratio of the contributions of the direct and compound scattering mechanisms to the investigated neutron cross sections. It can be seen from the data in Figs. 7 and 8 that for the levels 2_1^+ and 0_2^+ direct scattering becomes predominant

at neutron energies above 8 MeV, whereas for the level 4_1^+ this occurs above 10 MeV. For the level 2_1^+, the observed integrated inelastic-scattering cross sections at neutron energies below 10 MeV are shown in Fig. 10. The results of measurements of the different experimental groups (see Refs. 37–44 and 50–53) agree reasonably to within the indicated errors. Analyzing the observed asymmetry of the angular distributions of the scattered neutrons, we can trace the contribution of the direct transitions up to the neutron energy 3 MeV.

If we consider simultaneously the entire set of experimental data on the angular distributions of the neutrons scattered elastically and inelastically by the level 2_1^+, the optimal description of the observed cross sections is given by the coupled-channel model with the optical potential (20), in which the imaginary part is reduced by 20% when allowance is made for the $0_1^+-2_1^+$ level coupling ($\beta_2=0.48$), i.e., $W_s=5.7+0.52E_n$ is taken. The parameters of the integrated cross sections of direct and compound scattering of neutrons by the first 2^+ level corresponding to this choice are given in Fig. 10. When the set of parameters (23) is used, the cross section of direct scattering in the region of energies $E_n<6$ MeV is too large. This defect can be readily eliminated by changing the energy dependence of the imaginary part of the potential (23), and for the same choice of the imaginary potential the sets of parameters (20) and (23) become almost indistinguishable. If the number of coupled levels is increased, it is necessary to decrease even further the imaginary part of the optical potential, though mainly by decreasing the first term in the chosen parametrization of W_s, leaving the energy dependence essentially unchanged. Such a dependence is required, in particular, to describe the angular distributions shown in Figs. 6–8.

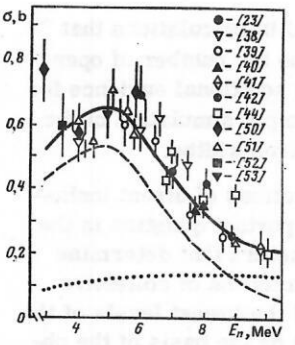

FIG. 10. Integrated cross section of inelastic scattering of neutrons by the 2^+ level of the ^{28}Si nucleus. The dotted curve shows the cross section of direct inelastic scattering; the broken curve, scattering through the compound nucleus; and the continuous curve, the total cross section of the two scattering mechanisms. The literature sources are indicated by square brackets.

If we go over to the range of neutron energies below 3 MeV, the main problem in the analysis here is the experimental determination of the average cross sections. In the experimental data, one can clearly see a fluctuation structure of the neutron cross sections (Fig. 11). Since the amplitude of the observed fluctuations is determined primarily by the resolution of the neutron spectrometers, it is a fairly complicated problem to correct the observed cross sections and the average cross sections obtained on their basis for the resonance absorption of neutrons in the target. Even more complicated is the construction of the angular distribution of the elastically and inelastically scattered neutrons averaged over the fluctuations, and at the present time we simply do not have sufficient experimental data for

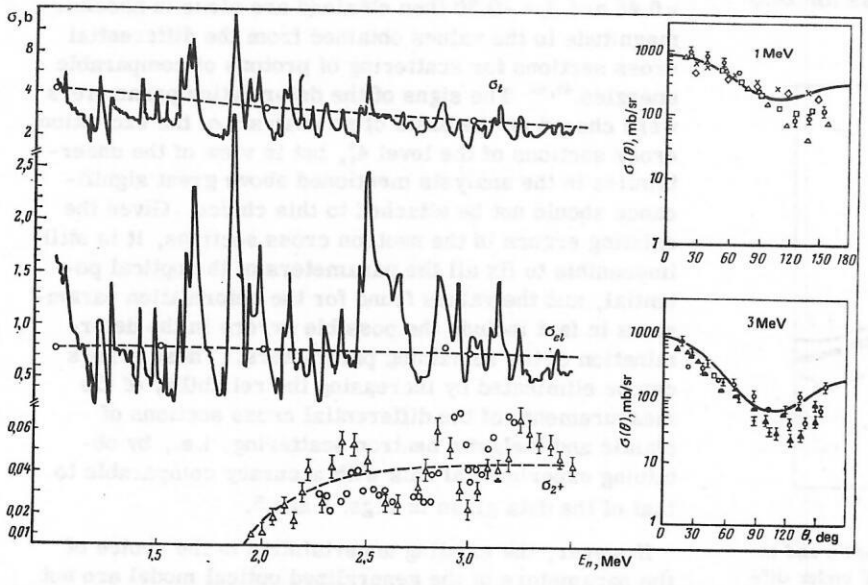

FIG. 11. Dependence of the total cross section σ_t, the elastic-scattering cross section $\sigma_{el}(\theta=20°)$, and the cross section of inelastic scattering by the first level $\sigma_{2_+}(\theta=60°)$ of the ^{28}Si nucleus on the neutron energy. The continuous curves are the cross sections measured in experiments with high energy resolution[54,55]; the broken curves are the description of the cross sections in the framework of the optical model. The inserts show the description of the angular distributions of elastically scattered neutrons; the experimental points are obtained by combining the results of measurements with different energy resolutions.[56]

such a construction. Nevertheless, comparing the existing data with optical-model calculations, we can conclude that there is qualitative agreement between the theoretical description and experiment (see Fig. 11). For a more rigorous quantitative analysis of the data and verification of the applicability of the different sets of optical-potential parameters, we need more accurate measurements of the angular distributions of elastically and inelastically scattered neutrons.

The direct mechanism of excitation of the lowest levels in a wide range of excitation energies was also investigated for the ^{32}S nucleus (Refs. 37–41, 50, and 57). For neutron energies above 7 MeV, the observed differential cross sections for inelastic scattering of neutrons by the level 2_1^+ ($Q = -2.23$ MeV) are shown in Fig. 12 together with the results of a theoretical description of the cross sections.[57] The optical-potential parameters in this description were determined by analyzing the differential cross sections of elastic and inelastic scattering of neutrons with energy 8 and 9 MeV,[39] and for the comparatively small extension of the range of energies of the incident particles it was not necessary to introduce any changes in these parameters. Since the spectrum of the low-lying levels of ^{32}S corresponds fairly well to the ideas of the vibrational model, the calculation of the direct transitions in the coupled-channel method was based on the vibrational $0_1^+ - 2_1^+$ level coupling scheme, and the deformation parameter $\beta_2 = 0.30$ was taken to be the same as in the description of the inelastic-scattering cross sections of charged particles.[48]

Similar experimental data and the results of the theoretical description of the cross sections for scattering of neutrons by the level 2_1^+ ($Q = -1.369$) of the ^{24}Mg nucleus are given in Fig. 13.[58] The calculations used the rotational $0_1^+ - 2_1^+$ level coupling scheme and equilibrium-deformation parameters $\beta_2 = 0.55$ and $\beta_4 = -0.05$. Since in ^{24}Mg the ratio $E_{4+}/E_{2+} = 3.02$ of the energies of the levels of the rotational band is much closer to the predictions of the rigid-rotator model than in Si, the differences between the equilibrium-deformation parameters extracted in different experiments are appreciably less.[45–47] But with the existing errors of the experimental data it is still impossible to establish whether the differences are due to the uncertainties in the choice of the optical-potential parameters or whether they characterize real differences in the isovector components of the intensity of direct excitation of levels when different particles are scattered.

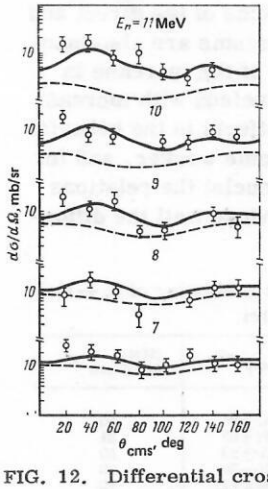

FIG. 12. Differential cross sections of inelastic scattering of neutrons by the first 2^+ level of the nucleus ^{32}S. The theoretical curves are the same as in Fig. 6.

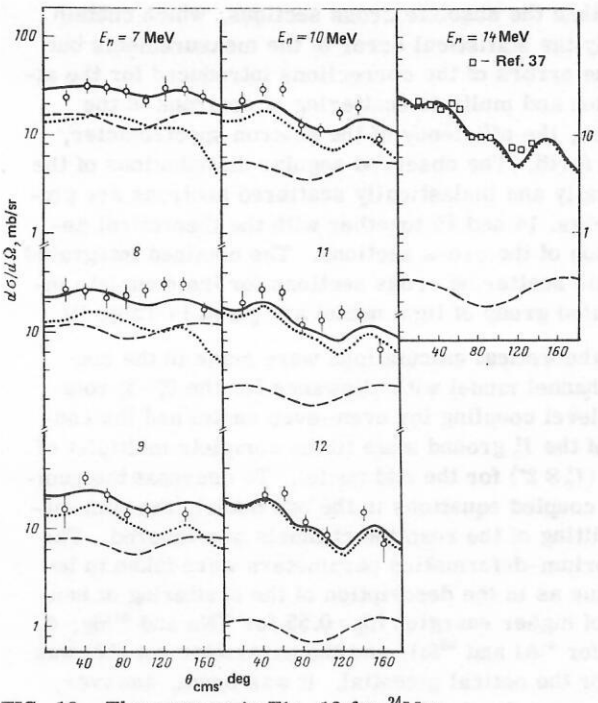

FIG. 13. The same as in Fig. 12 for ^{24}Mg.

It can be seen from the results of the calculations of the cross sections of the direct and compound mechanisms in Figs. 7, 12, and 13 that the contributions of the two mechanisms to the observed excitation cross sections of the first 2^+ level become approximately equal at neutron energies 7–9 MeV. At higher energies, direct excitation is dominant, and the integrated scattering cross section varies comparatively slowly with increasing energy of the neutrons. At neutron energies below 7 MeV, the behavior of the excitation functions is determined basically by scattering through the compound nucleus, but nevertheless it is impossible to ignore the contribution of the direct transitions when describing the cross sections for scattering by the collective levels in the entire range of energies to the threshold (see Fig. 10).

To investigate more fully the part played by direct transitions in the region of the maximum of the excitation functions of the low-lying levels, systematic measurements were made in Ref. 59 of the differential cross sections of elastic and inelastic scattering by the first levels of even–even and odd light nuclei for 3.4-MeV neutrons. To eliminate possible systematic errors of the experiment, the measurements of pairs of neighboring even–even and odd nuclei were made simultaneously. Under these conditions, the relative behavior of the differential scattering cross sections for the given pair of nuclei is determined with a much smaller

error than the absolute cross sections, which contain not only the statistical error of the measurements but also the errors of the corrections introduced for the attenuation and multiple scattering of neutrons in the samples, the efficiency of the neutron spectrometer, and so forth. The observed angular distributions of the elastically and inelastically scattered neutrons are given in Figs. 14 and 15 together with the theoretical description of the cross sections. The obtained integrated inelastic scattering cross sections for the complete investigated group of light nuclei are given in Table III.

The theoretical calculations were made in the coupled-channel model with allowance for the $0_1^+-2_1^+$ rotational level coupling for even–even nuclei and the coupling of the I_0^π ground state to the complete multiplet of levels $(I_0^\pi \otimes 2^+)$ for the odd nuclei. To decrease the number of coupled equations in the odd nuclei, the spin–orbit splitting of the reaction channels was ignored. The equilibrium-deformation parameters were taken to be the same as in the description of the scattering of neutrons of higher energies ($\beta_2 = 0.55$ for ^{23}Na and ^{24}Mg; $\beta_2 = 0.48$ for ^{27}Al and ^{28}Si), and the parameter set (19) was used for the optical potential. It was found, however, for the example of the even–even nuclei that approximately the same description of the observed differential cross sections can be obtained for the parameter set (20), and also the parameters used to describe the differential cross sections for scattering of neutrons with energy 7–12 MeV if the imaginary part of the potential in them is reduced by about 20%.

Overall, the results of the calculations agree rather well with the observed differential cross sections of inelastic neutron scattering (see Fig. 14), but much less well with the inelastic-scattering cross sections (see Fig. 15). The calculated integrated cross sections for inelastic scattering through the compound nucleus are always less than the experimental cross sections (see Table III), and this, like the observed general asymmetry of the angular distributions of the inelastically scattered neutrons, indicates a significant contribution of the direct scattering mechanism for the majority of the levels. The "fluctuations" of the angular distributions (see Fig. 15) still remain unclear. At the present time, it is difficult to decide whether they are due to ignored errors in the experimental data or reflect real fluctuations of the differential cross sections associated with the restricted interval of the averaged resonances of the compound nucleus.

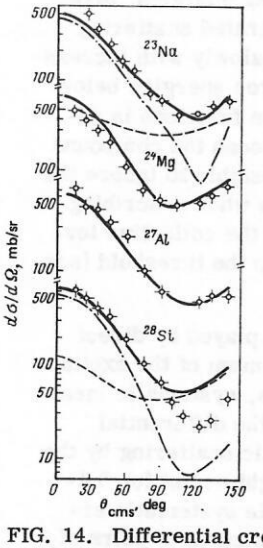

FIG. 14. Differential cross sections for inelastic scattering of 3.4-MeV neutrons. The broken curves show the cross section for scattering through the compound nucleus; the chain curves, the direct potential scattering in the coupled-channel model; and the continuous curves, the sum of the two scattering mechanisms.

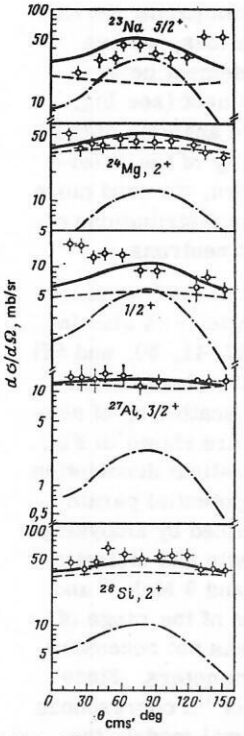

FIG. 15. The same as in Fig. 14 for inelastic scattering by the lowest levels. The notation is as in Fig. 14.

5. ANALYSIS OF THE EXCITATION FUNCTIONS OF LOW-LYING LEVELS OF MEDIUM NUCLEI

The general features that we have found above in the energy dependence of the contributions of the direct and compound neutron-scattering mechaisms are also manifested in heavier nuclei. Because of the increase in the level density of the compound nucleus with increasing mass number, the fluctuation effects in the behavior of the averaged cross sections become weaker, and for the majority of medium and heavy nuclei the relations of the statistical theory must reproduce well the differ-

TABLE III. Cross sections of inelastic scattering of 3.4-MeV neutrons by the first levels of light nuclei.

Target nucleus	Level energies, MeV	I^π	σ_{exp}, mb.	$\sigma_{calc}^{HFM}/\sigma_{exp}$, %
^{23}Na	0.439	5/2$^+$	443±94	55
^{24}Mg	1.369	2$^+$	511±93	91
^{27}Al	0.842	1/2$^+$	130±23	59
	1.013	3/2$^+$	170±30	88
^{28}Si	1.779	2$^+$	588±177	79
^{31}P	1.270	3/2$^+$	429±88	55

ential and integral excitation functions of isolated levels in the entire range of energies to the threshold. Analyzing the corresponding experimental data, we can investigate the part played by direct transitions and the energy dependence of the optical transmission coefficients at comparatively low energies of the incident neutrons. We shall discuss the results of such investigations for nuclei of the iron group, for which the most detailed experimental information is currently available.

The differential cross sections of elastic and inelastic scattering by the first 2^+ level of the ^{52}Cr nucleus for neutrons with energies 5, 6, and 7 MeV are shown in Fig. 16.[60] We also give the results of the theoretical description of the cross sections with the set (20) of the optical-potential parameters. As in the analogous calculations for light nuclei, the amplitude of the imaginary part of the potential (20) was decreased by about 20% in the coupled-channel model, and the quadrupole-deformation parameter $\beta_2 = 0.23$ was determined from the data on Coulomb level excitation.[28] This choice of the parameters ensures a good description of the observed asymmetry of the angular distributions of the inelastically scattered neutrons, and this permits a fairly reliable determination of the contribution of direct transitions (see Fig. 16). The contributions of the direct inelastic-scattering mechanism and scattering through the compound nucleus are approximately equal at energy 6 MeV of the incident neutrons. At lower energy, the integrated cross section of the direct transitions is slightly increased, whereas the cross section of the compound scattering mechanism increases comparatively rapidly.

The results of measurements of the integrated cross sections of inelastic scattering of neutrons by the first 2^+ level of ^{52}Cr are shown in Fig. 17. The significant spread of the experimental points at neutron energies below 3 MeV is due, in the first place, to methodological errors in the measurements of the different authors, and not to fluctuations in the averaged cross sections. With improvement in the experimental methods, this spread was partly eliminated, and the results of later measurements agree, as a rule, much better than the original experimental data.[60] The observed energy

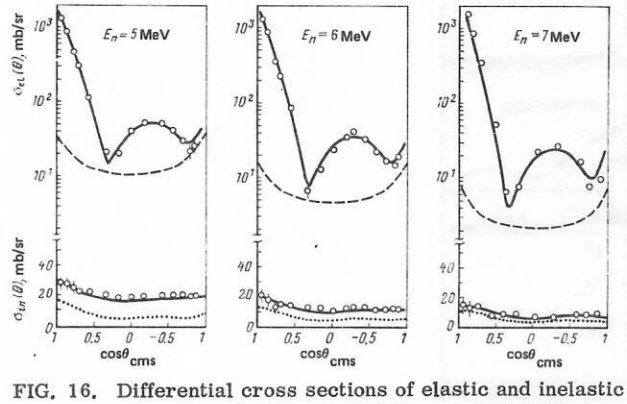

FIG. 16. Differential cross sections of elastic and inelastic scattering of neutrons by the level 2_1^+ ($Q = -1.435$ MeV) of the ^{52}Cr nucleus.[60] The theoretical curves are the same as in Fig. 6.

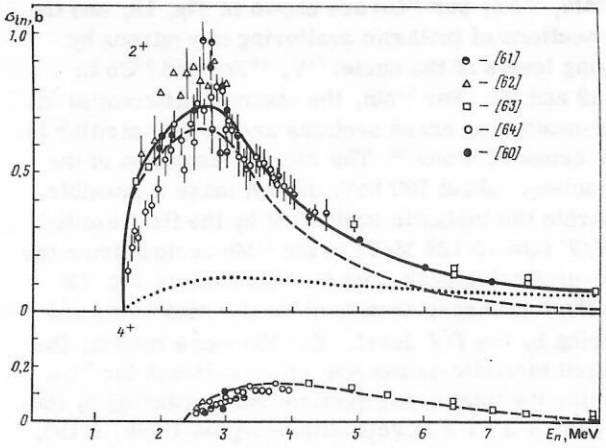

FIG. 17. Integrated cross section of inelastic scattering of neutrons by the levels 2_1^+ ($Q = -1.435$ MeV) and 4_1^+ ($Q = -2.370$ MeV) of the ^{52}Cr nucleus. The theoretical curves are the same as in Fig. 10, and the literature sources are indicated by the square brackets.

dependence of the inelastic-scattering cross sections can be well described by the theoretical curve obtained for the optical-potential parameters (20) and taking into account not only the scattering of neutrons through the compound nucleus but also the incoherent contribution of the direct transitions.[60]

A similar analysis of the experimental data on the differential and integral cross sections of excitation by neutrons of the lowest levels of the even–even nuclei ^{56}Fe, ^{58}Ni, and ^{60}Ni was made in Refs. 22 and 65–67. The conclusions of these papers regarding the contribution of the direct transitions and the choice of the optical-potential parameters do not differ significantly from the results obtained for ^{52}Cr. If we compare the excitation function of the first 2^+ level in the nuclei ^{52}Cr (see Fig. 17) and ^{28}Si (see Fig. 10), we can see that the energy dependences of the direct and compound components of the inelastic-scattering cross sections in light and medium nuclei are qualitatively similar. The observed quantitative differences between the direct scattering cross sections are due to the higher values of the quadrupole-deformation parameters of the light even–even nuclei, and the more rapid decrease in the cross sections of scattering through the compound nucleus with increasing neutron energy in medium nuclei reflects the general increase in the density of the excited levels.

Figure 17 also shows the experimental data on the excitation functions of the 4_1^+ level of the ^{52}Cr nucleus. The relations of the statistical theory describe fairly well the observed integrated scattering cross sections in the range of neutron energies from the threshold to 7 MeV, and it is only at higher energies that it becomes necessary to take into account the contribution of the direct transitions.

Systematic investigations of the part played by direct transitions at neutron energy 3.4 MeV were made in Ref. 68 for a set of neighboring even–even and odd nuclei of the iron group. The measured differential cross sections for elastic scattering of neutrons by the nuclei

^{51}V, ^{55}Mn, ^{56}Fe, and ^{59}Co are shown in Fig. 18, and the cross sections of inelastic scattering of neutrons by low-lying levels of the nuclei ^{51}V, ^{56}Fe, and ^{59}Co in Figs. 19 and 20. For ^{55}Mn, the obtained differential inelastic-scattering cross sections are largely similar to the ^{51}V cross sections.[68] The energy resolution of the spectrometer (about 100 keV) did not make it possible to separate the inelastic scattering by the first excited level $7/2^-$ ($Q = -0.126$ MeV) of the ^{55}Mn nucleus from the elastic-scattering peak, and for this nucleus Fig. 18 shows the total cross section of elastic scattering and scattering by the $7/2^-$ level. For the same reason, the measured inelastic-scattering cross sections for ^{59}Co determine the total cross sections for scattering by the three $3/2^-$, $9/2^-$, $3/2^-$ levels with energies 1.099, 1.190, and 1.291 MeV, respectively, and also by the $1/2^-$, $11/2^-$, and $5/2^-$ levels with energies 1.434, 1.460, and 1.471 MeV (see Fig. 20).

The observed cross sections were described theoretically in the coupled-channel model for the vibrational $0_1^+-2_1^+$ level coupling scheme in the nucleus ^{56}Fe and the equivalent coupling scheme of the ground state I_0^- to a multiplet of levels $(I_0^- \otimes 2^+)$ in odd nuclei. The optical-potential parameters (19) were used together with the dynamical-deformation parameters $\beta_2 = 0.23$ for ^{51}V and ^{55}Mn and $\beta_2 = 0.211$ for ^{59}Co. To shorten the amount of computing time in the odd nuclei, the spin–orbit splitting of the scattering channels was ignored. The results of the calculations agree fairly well with the measured differential cross sections of elastic and inelastic neutron scattering. The obtained integrated inelastic-scattering cross sections are given in Table IV. In the penultimate column of the table, we give the contribution of the compound scattering mechanism corresponding to the parameters of the statistical model given above. For the majority of the considered levels, the observed inelastic-scattering cross sections exceed the calculated cross sections for neutron scattering

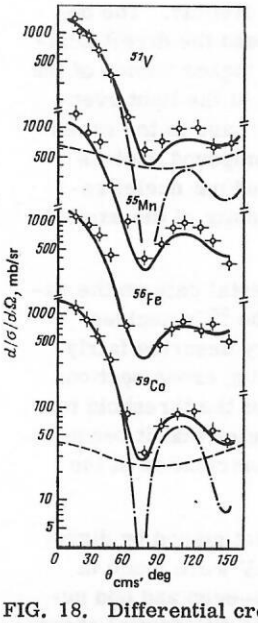

FIG. 18. Differential cross sections for elastic scattering of 3.4-MeV neutrons by nuclei of the iron group. The notation is the same as in Fig. 14.

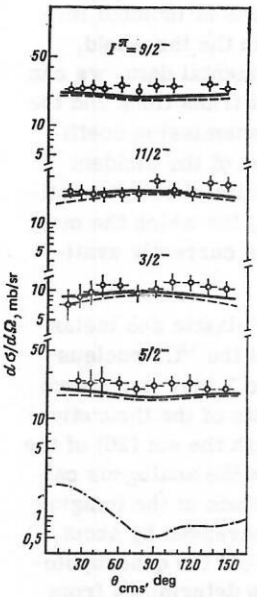

FIG. 19. Differential cross sections for inelastic scattering of 3.4-MeV neutrons by the lowest levels of the nucleus ^{51}V.

through the compound nucleus, and, together with the asymmetry of the angular distributions of the scattered neutrons, this result indicates that the direct processes make an important contribution. Estimates of this contribution are given in the last column of Table IV.[68] It can be seen that for the levels of the odd nuclei with high spin values the part played by the direct transitions is very appreciable, and it cannot be ignored in describing the excitation functions of these levels.

It should be noted that for the ^{56}Fe nucleus investigations of the angular distributions of inelastically scattered neutrons at energies of the incident neutrons below 3.5 MeV were also made in Refs. 69–71. Comparing the results of these papers, we see that there are appreciable discrepancies in the estimates of the contribution of the direct transitions. The discrepancies are due, on the one hand, to differences in the observed

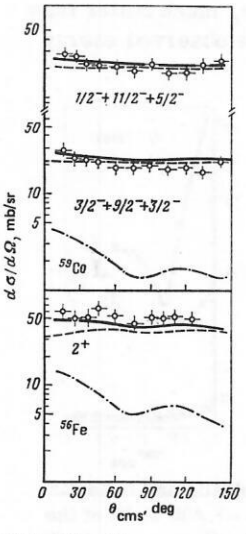

FIG. 20. The same as in Fig. 19 for ^{56}Fe and ^{59}Co.

TABLE IV. Cross sections for inelastic scattering of 3.4-MeV neutrons by low-lying levels of nuclei of the iron group.

Target nucleus	Level energies, MeV	I^π	σ_{exp}, mb	$\sigma_{calc}^{HFM}/\sigma_{exp}$, %	$\sigma_{calc}^{dir}/\sigma_{exp}$, %
^{51}V ($I_0^\pi = 7/2^-$)	0.319	$5/2^-$	287±32	80	4.6
	0.928	$3/2^-$	134±15	86	6.5
	1.609	$11/2^-$	265±29	90	7.5
	1.813	$9/2^-$	308±34	76	5.2
^{55}Mn ($I_0^\pi = 5/2^-$)	0.983	$9/2^-$	164±26	86	15.7
	1.289	$11/2^-$	102±16	88	29.2
	1.527	$3/2^-$	90±15	116	9.3
	1.884	$7/2^-$	81±19	112	—
^{56}Fe	0.845	2^+	643±114	72	12.4
^{59}Co ($I_0^\pi = 7/2^-$)	1.099	$3/2^-$	255±41	104	10.8
	1.190	$9/2^-$			
	1.291	$3/2^-$			
	1.434	$1/2^-$	273±44	91	11.2
	1.460	$11/2^-$			
	1.481	$5/2^-$			
	1.744	$7/2^-$	112±12	96	17.2

asymmetry of the angular distributions of the scattered neutrons and, on the other, to differences in the parameters of the optical potential. Analysis of the experiments with high resolution showed[71] that the determined fluctuations in the energy dependence of the cross sections remain even in the case of averaging over an interval of 200 keV, and, therefore, the differential cross sections measured at individual energy points still cannot be identified with the mean optical cross sections. If in choosing the parameters of the optical potential one attempts to describe the inelastic-scattering cross sections in a wide range of energies,[22,65] then for ^{56}Fe approximately the same estimate of the integrated cross section of direct inelastic scattering is obtained as for ^{52}Cr (see Fig. 17). Therefore, if to describe the excitation functions of low-lying levels of odd nuclei we use the parameter sets (20) or (22), we obtain for neutrons of energy 3.4 MeV contributions of the direct transitions that are 1.5–1.8 times higher than those given in Table IV. For a more reliable analysis of the part played by the direct processes, accurate measurements of the differential cross sections for scattering of neutrons by the levels of odd nuclei with spins $I_f^\pi > I_0^\pi$ would be of great interest.

In the description of the low-energy parts of the excitation functions of isolated levels, the agreement between the parameters of the optical model and the experimental values of the neutron strength functions is very important. The spherical optical model with optimal optical-potential parameters (19) or (20) reproduces only the global dependence of the neutron strength functions on the mass number,[5,9] but for individual nuclei the differences between the observed strength functions and the predictions of the optical model are very appreciable. As an example of these differences we can take the experimental and calculated strength functions of the nuclei of the iron group given in Table V. Although the transition from the single-channel optical model to the coupled-channel model improves on the whole the description of the experimental data, for many nuclei the discrepancy between the calculations and the experiments is still appreciable in the latter.

TABLE V. Neutron strength functions of even–even nuclei of the iron group (in units of 10^{-4}).

Target nucleus	Spherical optical model		Coupled-channel model		Experiment[72]	
	s_0	s_1	s_0	s_1	s_0	s_1
^{50}Cr	3.64	1.25	4.90	1.34	3.6±0.8	0.33±0.12
^{52}Cr	5.32	0.96	4.82	1.15	2.5±0.9	0.52±0.12
^{54}Cr	—	—	3.05	1.17	2.8±1.0	—
^{54}Fe	—	—	5.18	0.83	8.7±2.4	0.58±0.11
^{56}Fe	4.62	0.80	3.05	0.93	2.6±0.6	0.45±0.05
^{58}Fe	—	—	2.64	0.88	3.6±1.2	0.6±0.2
^{58}Ni	—	—	3.01	0.81	2.8±0.6	0.5±0.1
^{60}Ni	3.90	0.74	2.53	0.81	2.7±0.6	0.3±0.1
^{62}Ni	—	—	2.45	0.80	2.8±0.7	0.3±0.1
^{64}Ni	—	—	2.43	0.79	2.9±0.8	0.6±0.2

Similar discrepancies for a larger group of nuclei were discussed in Refs. 72–74. An interpretation of these discrepancies can be sought in the theory of doorway states[75] or in other formulations of the microscopic theory of nuclear reactions,[76] but irrespective of the existence of a more fundamental explanation of the nature of the observed effects, the experimental values of the the strength functions must undoubtedly be taken into account in a phenomenological analysis of the excitation functions of low-lying levels of definite nuclei.

The part played by the neutron strength functions in describing the near-threshold behavior of the excitation functions of the first levels of even–even nuclei can be seen from the results presented in Fig. 21. Calculations with transmission coefficients $T_{lj}(E_n)$ corresponding to the spherical optical model give a significantly too large cross section for inelastic scattering of neutrons by the first 2^+ level. But if renormalized transmission coefficients are introduced in the calculations—chosen such that at neutron energies below 100 keV they correspond to the experimental strength functions (s_0 for even partial waves and s_1 for odd), and at neutron

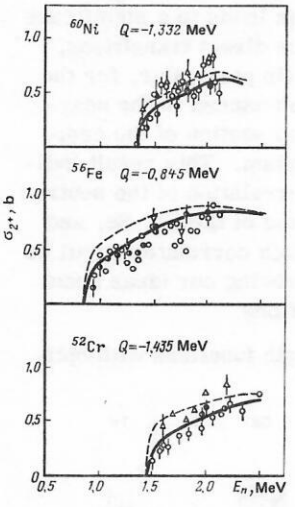

FIG. 21. Description of the near-threshold parts of the excitation functions of the first 2^+ levels of even–even nuclei of the iron group for the transmission coefficients of the coupled-channel model (broken curves) and for the transmission coefficients "tied" to the experimental values of the neutron strength functions (continuous curves). The experimental points are obtained by combining measurements of different authors (Refs. 60–64, 66, 70, and 71).

energies 2–3 MeV go over smoothly into the transmission coefficients of the generalized optical model—the description of the near-threshold part of the excitation functions is significantly improved (see Fig. 21). A similar effect can be achieved by the choice of the optical-potential parameters V_v and W_s.[74] In this case, the energy dependence of the optical-model parameters in the region of low energies ($E_n \lesssim 3$ MeV) will be very different from the dependence observed at higher energies.[77] It should be noted that a "tying" of the transmission coefficients to the resonance values of the strength functions is, as a rule, also necessary for consistent description of the total neutron cross sections and cross sections of radiative capture of neutrons at low energies $E_n \lesssim 1$ MeV.[63]

We encounter an effect of the same nature, although manifested differently, in the analysis of the near-threshold parts of the functions of excitation by neutrons of the first levels of heavier nuclei.[78] Figure 22 shows the observed cross sections for inelastic scattering of neutrons at energy 300 keV above the threshold of the 2^+ level, and also the results of the theoretical description of these cross sections. The transmission coefficients used in the theoretical calculations were determined in the coupled-channel model with optical-potential parameters $V_v = 53–54$ MeV and $W_s = 2–3$ MeV, which give optimal description of the neutron strength functions of the s and p resonances. For the majority of the nuclei, the inelastic-scattering cross sections are also reproduced reasonably for such a choice of the parameters (see Fig. 22). However, for some Ge, Se, and Te isotopes an appreciable discrepancy between the calculations and the experimental data is observed. A more detailed analysis of such isotopes showed that agreement with experiment can be achieved by taking into account the coupling of a sufficiently large number of inelastic-scattering channels and a simultaneous decrease in the imaginary part W_s of the optical potential to 1 MeV.[78] This leads to a significant increase in the contribution of the direct transitions, and for individual partial waves (in particular, for the p wave) the contribution may even exceed in the near-threshold region the partial cross section of the compound neutron-scattering mechanism. This result indicates the possibility of strong correlation of the neutron widths of the p resonances in some of the Ge, Se, and Te isotopes. Further study of such correlations will be of considerable interest for improving our ideas about the mechanisms of nuclear reactions.

Since calculations of the strength functions with optimal sets of the optical-potential parameters still on the average reproduce quite well the general behavior of the transmission coefficients, it is natural that in many nuclei we do not observe significant deviations of the experimental excitation functions from the theoretical description obtained with a "common" optical potential. However, for nuclei in which the above features of the energy dependence of the excitation functions of the first levels are manifested and require for their explanation an appreciable change in the parameters of the potential in the low-energy region, one would expect similar effects in the excitation functions of all the following levels, including the region of unresolved levels. The experimental study of such effects could give information about the differences between the optical potentials for the ground and excited states of nuclei. Very interesting results in this direction were obtained in Ref. 79, which demonstrated the possibility of extracting the energy dependence of the cross section for absorption of neutrons by a highly excited nucleus ($U \approx 8–12$ MeV) from analysis of the low-energy part of the neutron spectra of the (p, np') reaction on Ni, Zr, and Sn nuclei. The obtained cross sections indicate an appreciable difference between the absorption of neutrons in an excited and nonexcited nucleus, but as yet the data are too few to draw on their basis unambiguous conclusions about the change in the optical potential in highly excited nuclei.

Some ideas about the expected differences between the transmission coefficients for the ground states and first excited states of nuclei can be obtained from the calculations of the neutron strength functions in the coupled-channel model.[11,12] In the framework of this model, one can take as the entrance channel any of the considered definitely open scattering channels and then follow the resulting changes in the strength functions or transmission coefficients. As an example, Table VI gives the results of calculation of the transmission coefficients of s and p neutrons for the ground and first excited states of the nuclei ^{56}Fe and ^{92}Zr at neutron energies 0.1 and 1.0 MeV.[12] At low neutron energies (below 0.1 MeV) the differences between the transmission coefficients are very appreciable, but they decrease significantly with increasing energy of the incident neutrons.

On the basis of such calculations it can be concluded that the traditional procedure in which the transmission coefficients are taken to be the same for the ground and excited states of nuclei can distort in a certain manner

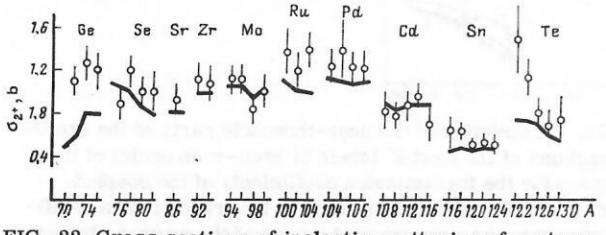

FIG. 22. Cross sections of inelastic scattering of neutrons at energy 300 keV above the excitation threshold of the 2_1^+ level (open circles) and their theoretical description in the coupled-channel model (continuous curves).

TABLE VI. Transmission coefficients T_{lj} for the ground and the first excited state of nuclei.

Target nucleus	E_n, MeV	State	$T_{0\,1/2}$	$T_{1\,1/2}$	$T_{1\,3/2}$
^{56}Fe $\beta_2 = 0.24$	0.1	Ground	0.526	0.0135	0.0100
		Excited	0.742	0.0086	0.0074
	1.0	Ground	0.832	0.158	0.140
		Excited	0.735	0.113	0.110
^{92}Zr $\beta_2 = 0.13$	0.1	Ground	0.089	0.143	0.282
		Excited	0.068	0.074	0.164
	1.0	Ground	0.215	0.946	0.964
		Excited	0.180	0.758	0.873

the results of the analysis of the low-energy parts of the excitation functions of levels, and these distortions may be very appreciable in the region of the maxima of the maxima of the corresponding strength functions. Therefore, the inclusion of these effects in the description of the neutron cross sections is, although it does complicate the analysis, necessary when one is considering the ever more accurate experimental data.

CONCLUSIONS

The main results of the above investigations into the scattering of neutrons by low-lying levels of light and medium nuclei can be briefly summarized as follows.

1. For the analysis of the differential cross sections of elastic neutron scattering, the transition from the single-channel optical model to the generalized coupled-channel model eliminates a large amount of the spurious fluctuations of the optical-potential parameters. In the framework of the generalized optical model, one can follow much better the energy and isotopic variations in the depth of the potential and, in particular, the significant difference between the energy dependence of the imaginary part of the optical potential at neutron energies up to 15 MeV and in the region of higher energies.

2. Accurate measurements of the differential cross sections of inelastic scattering of neutrons by the lowest collective levels of even–even nuclei are a very effective means for investigating the structural differences between the isoscalar and isovector components of nuclear excitations. Such differences have hitherto been studied only for the lowest quadrupole excitations of near-magic nuclei with a closed proton, $Z=50$, or neutron, $N=50$, shell, and considerable interest attaches to investigation of the analogous effects in the excitation of higher levels.

3. The direct inelastic-scattering mechanism makes an important contribution to the observed cross sections for excitation of the lowest collective levels even at comparatively low neutron energies $E_n \lesssim 3$ MeV. Allowance for the direct transitions reduces the integrated cross sections for neutron scattering by the compound nucleus and changes accordingly the transmission coefficients for the different partial waves. Analysis of the excitation functions of the 4_1^+ and 0_2^+ levels of ^{28}Si demonstrates the important part played by these changes in the consistent description of the experimental data. Study of these changes for a larger group of nuclei will facilitate the further improvement in the methods of theoretical analysis of the cross sections of nuclear reactions, and also the more accurate determination of the parameters of the optical potential, which is used for many practical applications of neutron physics.

4. In the description of the near-threshold parts of the level excitation functions it is in principle important to take into account the individual structural irregularities in the variation of the neutron strength functions. So far, the influence of such irregularities has been followed only for a limited number of the lowest levels of even–even nuclei. The extension of this direction of investigation may become very fruitful for the study of the differences between the optical potentials for the ground and excited states of nuclei.

We are very grateful to I. A. Korzh, G. N. Lovchikova, and N. M. Pravdivyĭ for numerous fruitful discussions of the questions considered in this paper.

[1]J. M. Blatt and V. F. Weisskopf, Theoretical Nuclear Physics, Wiley, New York (1952) [Russian translation published by Izd. Inostr. Lit., Moscow (1954)].
[2]A. M. Lane and R. G. Thomas, "R-matrix theory of nuclear reactions," Rev. Mod. Phys. **30**, 257 (1958) [Russian translation published as a book by Izd. Inostr. Lit., Moscow (1960)].
[3]N. Austern, Direct Nuclear Reaction Theories, Wiley Interscience, New York (1970).
[4]J. R. Lynn, Theory of Neutron Resonance Reactions, Clarendon Press, Oxford (1968).
[5]P. E. Hodgson, The Optical Model of Elastic Scattering, Clarendon Press, Oxford (1963) [Russian translation published by Atomizdat, Moscow (1960)].
[6]G. I. Marchuk and V. E. Kolesov, Primenenie chislennykh metodov dlya rascheta neĭtronnykh sechenii (Use of Numerical Methods to Calculate Neutron Cross Sections), Atomizdat, Moscow (1966).
[7]A. Prince, Nuclear Theory in Neutron Nuclear Data Evaluation, Vol. 1, IAEA-190, Vienna (1976), p. 31.
[8]A. Bohr and B. R. Mottelson, Nuclear Structure, Vol. 2, Benjamin, Reading, Mass. (1975) [Russian translation published by Mir., Moscow (1977)].
[9]T. Tamura, Rev. Mod. Phys. **37**, 679 (1965).
[10]A. V. Ignatyuk, V. P. Lunev, and V. S. Shorin, Vopr. At. Nauki Tekh., Ser. Yad. Konst. No. 13, 59 (1974).
[11]Ch. Dunford, H. Fenech, and J. T. Reynolds, Phys. Rev. **177**, 1395 (1969).
[12]A. V. Ignatyuk and V. P. Lunev, in: Neĭtronnaya fizika (Neutron Physics), Part 1, TsNIIAI, Moscow (1980), p. 77.
[13]P. Moldauer, Rev. Mod. Phys. **36**, 1079 (1964).
[14]N. M. Hoffmann *et al.*, Ann. Phys. (N. Y.) **90**, 403 (1975).
[15]P. Moldauer, Nuclear Theory for Applications, IAEA-SMR-43, Trieste (1980), p. 165.
[16]J. Tepel, H. Hoffmann, and H. Weidenmüller, Phys. Lett. **B49**, 1 (1974).
[17]F. D. Becchetti and G. W. Greenlees, Phys. Rev. **182**, 1190 (1969).
[18]B. Holmqvist and T. Wielding, Nucl. Phys. **A188**, 24 (1972).
[19]B. Holmqvist and T. Wielding, J. Nucl. Energy **27**, 543 (1973).
[20]M. V. Pasechnik, I. A. Korzh, and I. E. Kashuba, in: Neĭtronnaya fizika (Neutron Physics), Part 1, Naukova Dumka, Kiev (1972), p. 253.
[21]D. E. Bainum *et al.*, Nucl. Phys. **A311**, 492 (1978); J. Rapaport *et al.*, Nucl. Phys. **A341**, 56 (1980).
[22]S. Tanaka, in: Proc. of the EANDC Topical Discussion on Critique of Nuclear Models and their Validity in Evaluation of Nuclear Data, JAERI-5984 (1975), p. 212.
[23]S. Tanaka *et al.*, in: Nuclear Data for Reactors, Vol. 2, IAEA, Vienna (1970), p. 317.
[24]J. Rober and J. Brandenberger, Phys. Rev. **163**, 1077 (1967).
[25]J. P. Delaroche, Ch. Lagrange, and J. Salvy, in: Nuclear Theory in Neutron Nuclear Data Evaluation, Vol. 1, IAEA-190, Vienna (1976), p. 251.
[26]A. Ferguson *et al.*, in: Proc. of the Intern. Conf. on Interaction of Neutrons with Nuclei, Lowell (1976), p. 204.
[27]G. Haouat, in: Neutron Induced Reactions (Proc. of the Second Intern. Symposium in Smolenice), VEDA, Bratislava (1980), p. 333.
[28]P. H. Stelson and L. Grodzins, Nucl. Data **A1**, 21 (1965).
[29]C. J. Veje, K. Dan. Vidensk. Selsk, Mat.-Fys. Medd. **35**,

No. 1 (1966).
[30]V. R. Brown and V. A. Madsen, Phys. Rev. C 11, 1298 (1975); V. A. Madsen, V. R. Brown, and J. D. Anderson, Phys. Rev. C 12, 1205 (1975).
[31]R. W. Finlay *et al.*, Nucl. Phys. A338, 45 (1980).
[32]A. I. Blokhin, A. V. Ignatyuk, and V. P. Lunev, in: Neĭtronnaya fizika (Neutron Physics), Part 1, TsNIIAI, Moscow (1980), p. 89.
[33]J. Lachkar *et al.*, Phys. Rev. C 14, 933 (1976).
[34]M. Matoba *et al.*, Nucl. Phys. A325, 389 (1979).
[35]L. Compte *et al.*, Nucl. Phys. A284, 123 (1977).
[36]V. I. Strizhak *et al.*, Fizika bystrykh neĭtronov (Physics of Fast Neutrons), Atomizdat, Moscow (1977), Chap. 2.
[37]R. L. Clarke and W. G. Cross, Nucl. Phys. 53, 177 (1964); P. W. Martin *et al.*, Nucl. Phys. 61, 524 (1965); P. H. Stelson *et al.*, Nucl. Phys. 68, 97 (1965).
[38]M. K. Drake *et al.*, Nucl. Phys. A128, 209 (1969).
[39]W. E. Kinney and F. G. Perey, ORNL-4517 and 4539 (1970).
[40]J. D. Brandenberger, A. Mittler, and M. T. McEllistrem, Nucl. Phys. A196, 65 (1972).
[41]A. W. Obst and J. L. Weil, Phys. Rev. C 7, 1076 (1973).
[42]D. E. Velkley *et al.*, Phys. Rev. C 9, 2181 (1974).
[43]W. Pilz *et al.*, in: Neutron Induced Reactions, VEDA, Bratislava (1980), p. 127; in: Proc. of the Ninth Intern. Symposium on Interaction of Fast Neutrons with Nuclei, ZfK-410, Dresden (1980), p. 57.
[44]D. Schmidt, D. Seeliger, and T. Streil, in: Proc. of the Tenth Intern. Symposium on Interaction of Fast Neutrons with Nuclei, ZfK-459, Dresden (1981), p. 164; T. Streil, Dr. Thesis, TU Dresden (1981).
[45]M. M. Aleonard *et al.*, Nucl. Phys. A146, 90 (1970); F. Huang and D. K. McDaniels, Phys. Rev. C 2, 1342 (1970).
[46]M. C. Mermaz *et al.*, Phys. Rev. 187, 1466 (1969); H. Rebel *et al.*, Nucl. Phys. A182, 145 (1972).
[47]A. G. Blair *et al.*, Phys. Rev. C 1, 444 (1970).
[48]R. De Swinarski *et al.*, Nucl. Phys. A261, 111 (1976).
[49]E. De Leo *et al.*, Phys. Rev. C 19, 646 (1979).
[50]G. A. Petitt *et al.*, Nucl. Phys. 79, 231 (1966).
[51]W. E. Knitter and M. Coppola, Z. Phys. 207, 56 (1967).
[52]Th. Schweitzer *et al.*, Kernenergie 6, 174 (1977).
[53]I. A. Korzh, V. A. Mishchenko, and I. E. Sanzhur, Ukr. Fiz. Zh. 25, 109 (1980).
[54]S. Cierjacks *et al.*, KfK-1000, Karlsruhe (1968).
[55]I. Schouky, KfK-2503, Karlsruhe (1977).
[56]D. Hermsdorf and L. Neumann, in: Proc. of the Ninth Intern. Symposium on Interaction of Fast Neutrons with Nuclei, ZfK-410, Dresden (1980), p. 147.
[57]M. Adel-Fawzy *et al.*, in: Proc. of the Ninth Intern. Symposium on Interaction of Fast Neutrons with Nuclei, ZfK-410, Dresden (1980), p. 60.
[58]H. Förtsch, Dr. Thesis, TU Dresden (1981).
[59]T. Schweitzer, D. Seeliger, and S. Unolzer, in: Proc. of the Eighth Intern. Symposium on Interaction on Fast Neutrons with Nuclei, ZfK-382, Dresden (1979), p. 125.
[60]I. A. Korzh *et al.*, Yad. Fiz. 35, 1097 (1982) [Sov. J. Nucl. Phys. 35, 641 (1982)].
[61]D. M. Van Patter *et al.*, Phys. Rev. 128, 1246 (1962).
[62]D. L. Broder *et al.*, At. Energ. 18, 645 (1964).
[63]W. E. Kinney and F. G. Perey, ORNL-4806 (1974).
[64]P. T. Karatzas *et al.*, Nucl. Sci. Eng. 67, 34 (1978).
[65]V. M. Bychkov *et al.*, Vopr. At. Nauki Tekh. Ser. Yad. Konst. No. 19, 110 (1975).
[66]A. Smith *et al.*, Nucl. Sci. Eng. 72, 293 (1979).
[67]I. A. Korzh *et al.*, At. Energ. 50, 398 (1981).
[68]A. H. Mohamed *et al.*, in: Proc. of the Ninth Intern. Symposium on Interaction of Fast Neutrons with Nuclei, ZfK-410, Dresden (1980), p. 34.
[69]K. Tsukada, Nucl. Phys. A125, 641 (1969).
[70]I. A. Korzh *et al.*, Ukr. Fiz. Zh. 22, 87 (1977).
[71]A. Smith and P. Guenther, Nucl. Sci. Eng. 73, 186 (1980).
[72]S. F. Mughabghab, M. Divadeenam, and N. E. Holden, Neutron Cross Sections, Vol. 1, Academic Press, New York-London (1981).
[73]K. N. Müller and G. Rohr, Nucl. Phys. A164, 97 (1971).
[74]C. M. Newstead, J. Delaroche, and B. Canvin, in: Statistical Properties of Nuclei, Plenum Press, New York (1972), p. 367.
[75]H. Feshbach, A. K. Kerman, and R. H. Lemmer, Ann. Phys. (N. Y.) 41, 230 (1967).
[76]Yu. V. Adamchuk and V. K. Sirotkin, Yad. Fiz. 26, 495 (1977) [Sov. J. Nucl. Phys. 26, 262 (1977)].
[77]V. Benzi, F. Fabbri, and G. Reffo, in: Proc. of the EANDC Topical Discussion on Critique of Nuclear Models and their Validity in Evaluation of Nuclear Data, JAERI-5984 (1975), p. 83.
[78]V. P. Efrosinin, R. M. Musaelyan, and V. I. Popov, Yad. Fiz. 29, 631 (1979) [Sov. J. Nucl. Phys. 29, 326 (1979)]; E. S. Konobeevskiĭ and V. I. Popov, Preprint R-0155 [in Russian], Institute of Nuclear Research, USSR Academy of Sciences, Moscow (1980).
[79]G. R. Rao *et al.*, Phys. Rev. C 7, 733 (1973).

Translated by Julian B. Barbour